High Resolution SAR (Radar) Interferometry at L- und S-Band

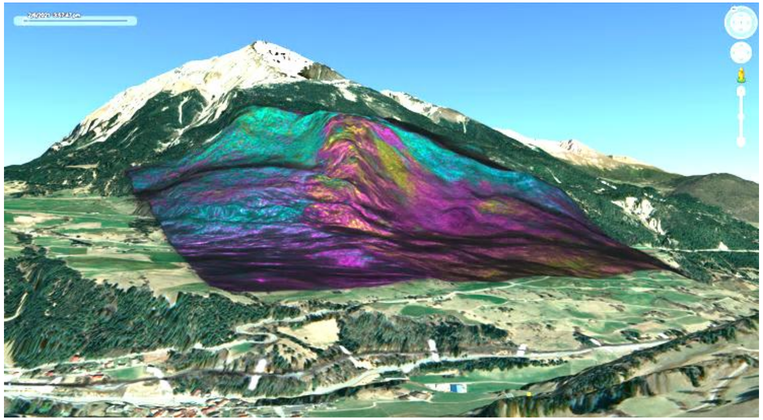

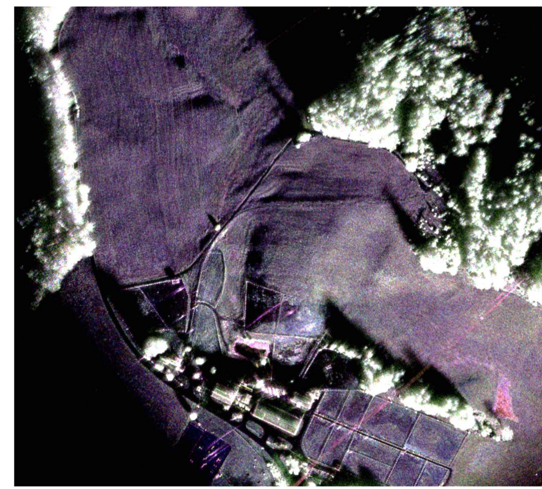

Charles Werner and Othmar Frey, Silvan Leinss, and Tobias Batt
Gamma Remote Sensing AG, Worbstrasse 225, Gümligen, Switzerland
http://www.gamma-rs.ch

GAMMA REMOTE SENSING

Electromagnetic Spectrum

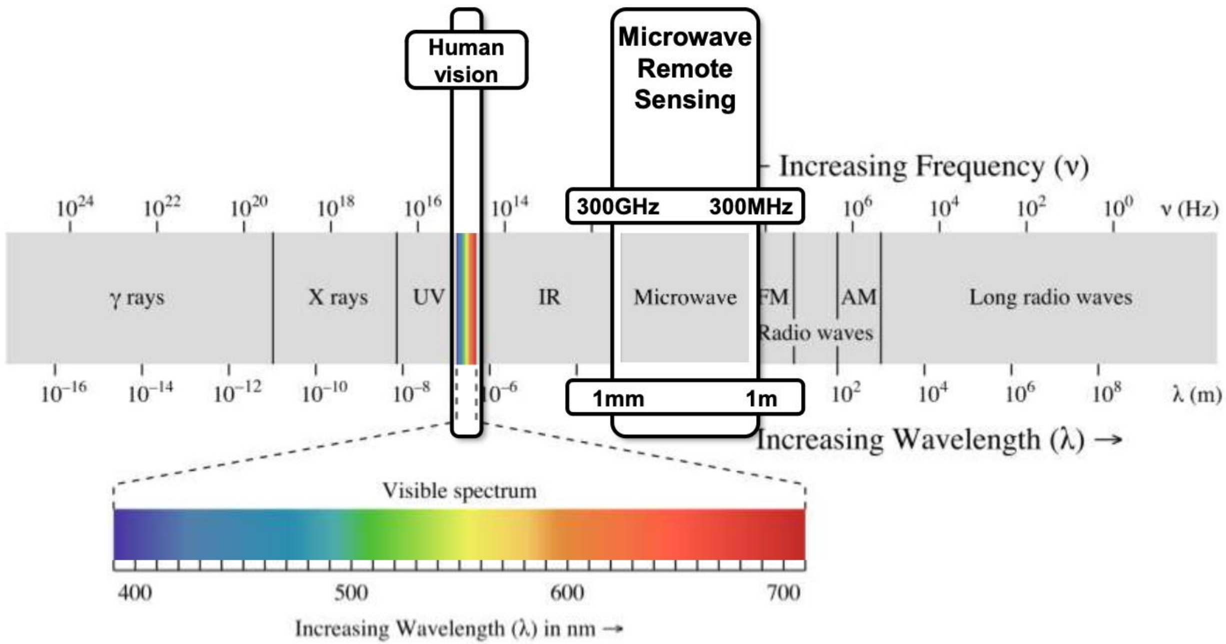

Atmospheric Transmission of Microwaves

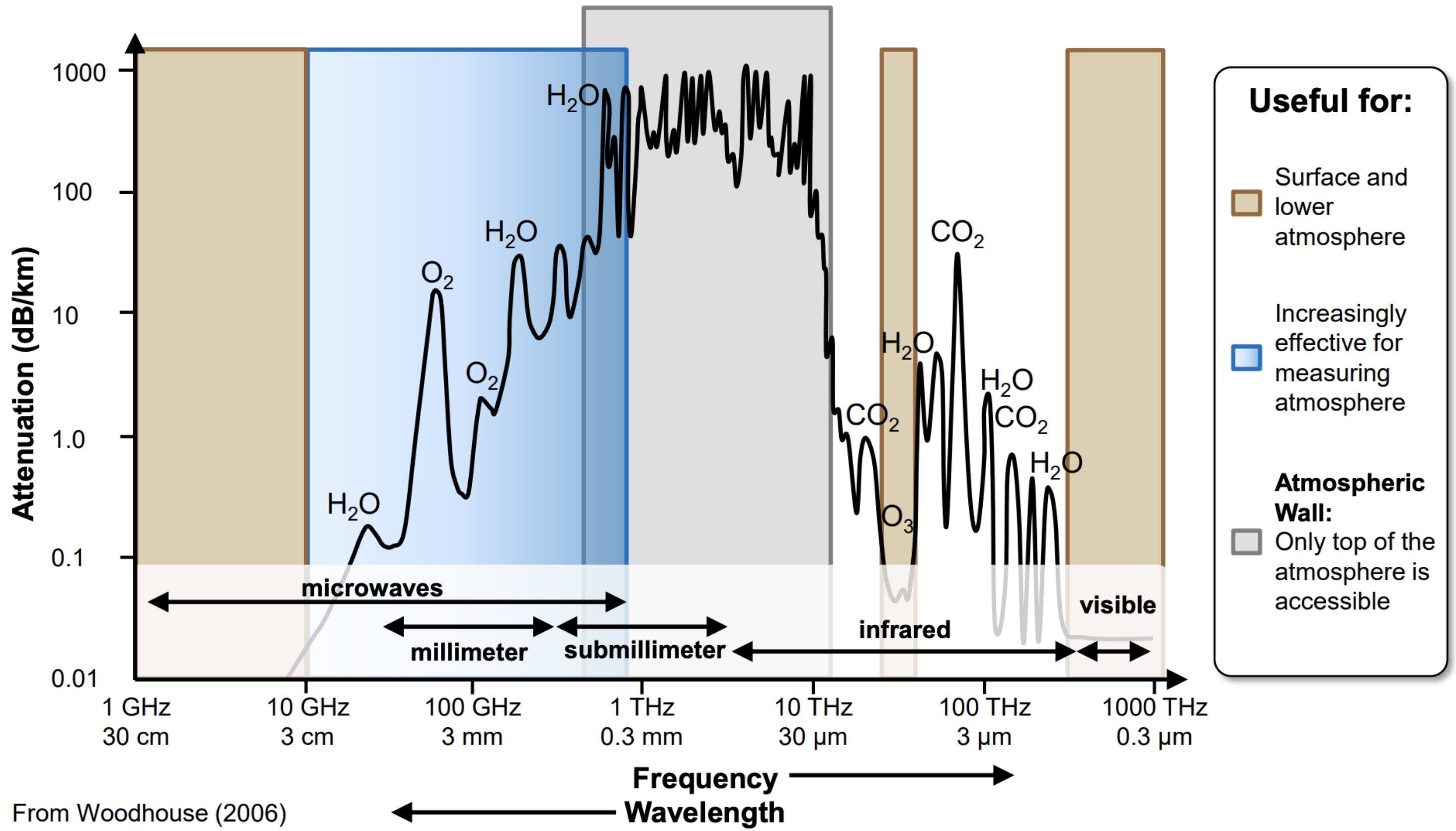

From Woodhouse (2006)

Active Microwave Systems (RADAR)

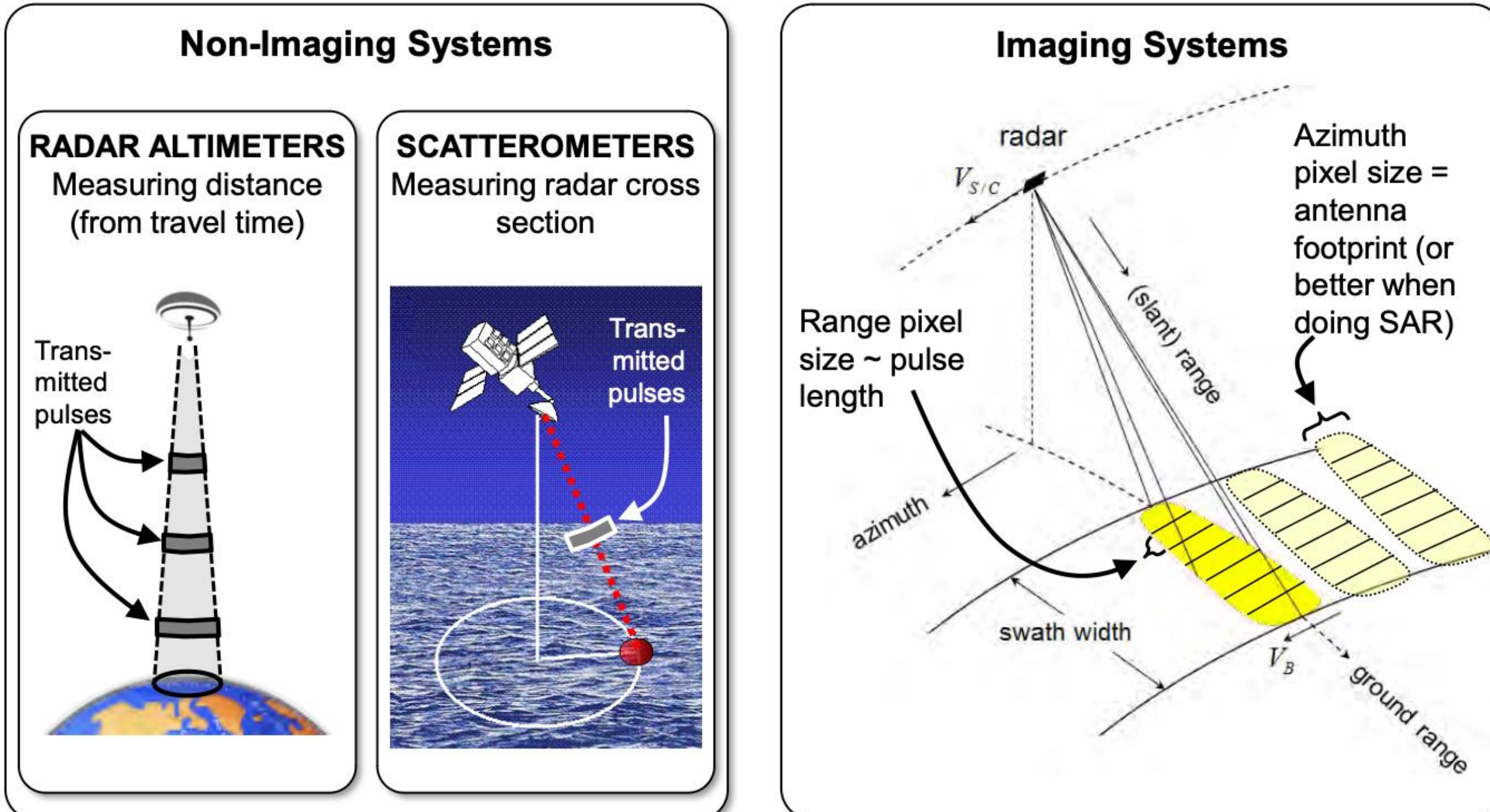

Synthetic Aperture Radar Imaging Systems

- The radar transmits electromagnetic waves in the microwave part of the spectrum. Operational SAR instruments operate in the approximate frequency range of 0.4 GHz to 95 GHz, with some experimental systems exploring both higher and lower parts of the spectrum. The radar signal wavelengths are in the range: 75 cm to 3.1 mm
- SAR systems must be coherent, meaning that they measure not just the intensity of the scattered radiation (such as an optical camera), but also the phase. Knowing the both phase and amplitude of the field in permits calculation of field values as a function of space and time.
- What is the phase?

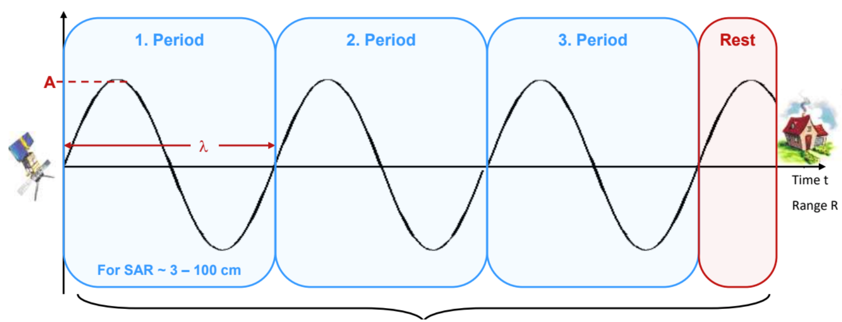

$$\phi = \frac{-4\pi R}{\lambda}$$

$$z = a_i e^{j\phi}$$

- Recording the phase permits computational propagation the field backwards and forwards in time. Focusing the SAR image is equivalent to propagation of the measured field back to where it scattered from the surface.

Exciting Developments in SAR:

New Sensors, Free-And-Open Regularly-Sampled Data, Application-Ready Data (ARD) Products

Sentinel-1

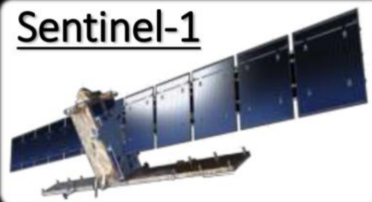

Frequency:
C-band

Launch Date:
2015 & 16

NISAR

NASA - ISRO SAR Mission

Frequency:
L-band

Launch Date:
January 2024

TanDEM-L

Frequency:
L-band

Launch Date:
TBD

October 2016
November
December
January 2017
February
March
April
May

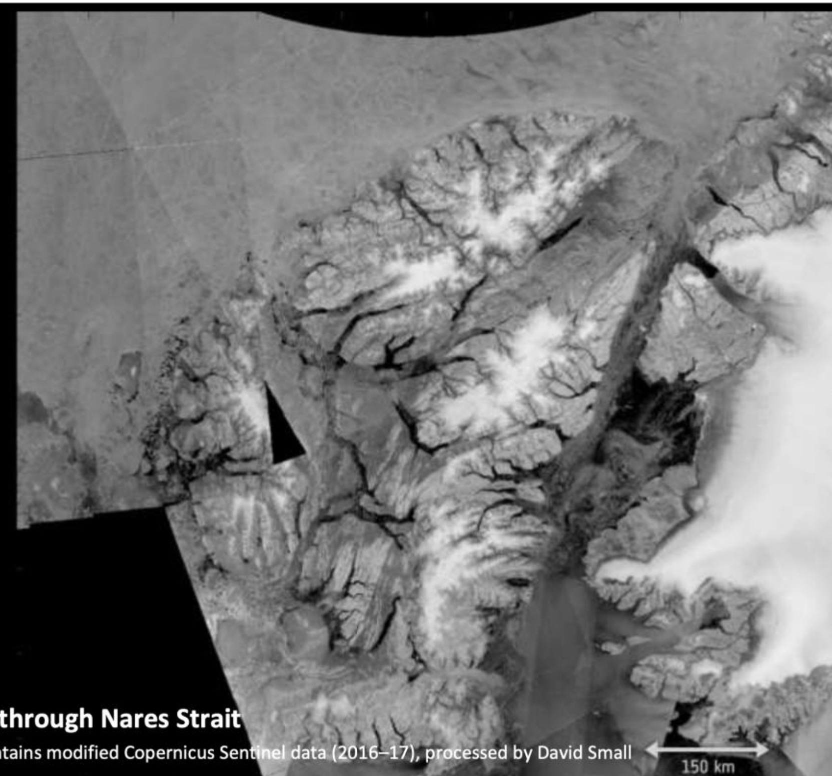

Arctic Sea Ice Export through Nares Strait

Side-Looking Imaging Radar Geometry

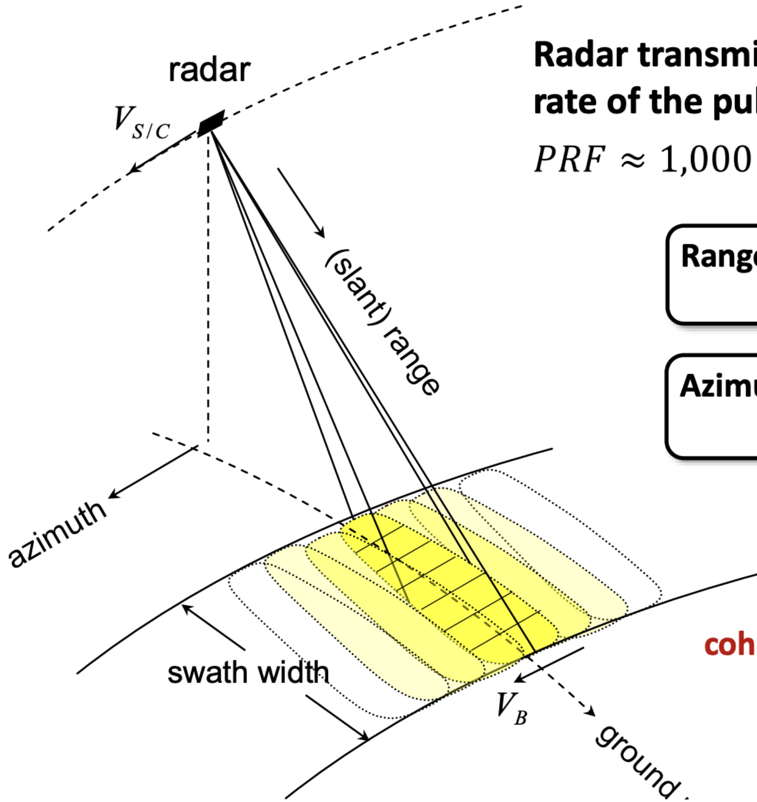

Radar transmits pulses and receives echoes at the rate of the pulse-repetition frequency (PRF):

$PRF \approx 1{,}000 - 4{,}000Hz$

Range resolution:	defined by pulse width (radar principle)

Azimuth resolution:	scanning in flight direction at $V_{S/C}$

coherent imaging: complex-valued pixels contain amplitude (brightness) and phase information

Radar Interferometry Concept and Applications

Radar interferometry consists of interfering two radar images with a small baseline. Both the magnitude and phase of the image are required.

- Topography can be precisely recovered using the phase information thus allowing a 3-dimensional reconstruction of the viewed scene.
- Deformation along the Line of Sight (LOS) can measured using phase, given that the radar scatterers are temporally correlated.
- Temporal Decorrelation can also be measured and used for classification of the scattering surface or to detect landslides, or avalanches

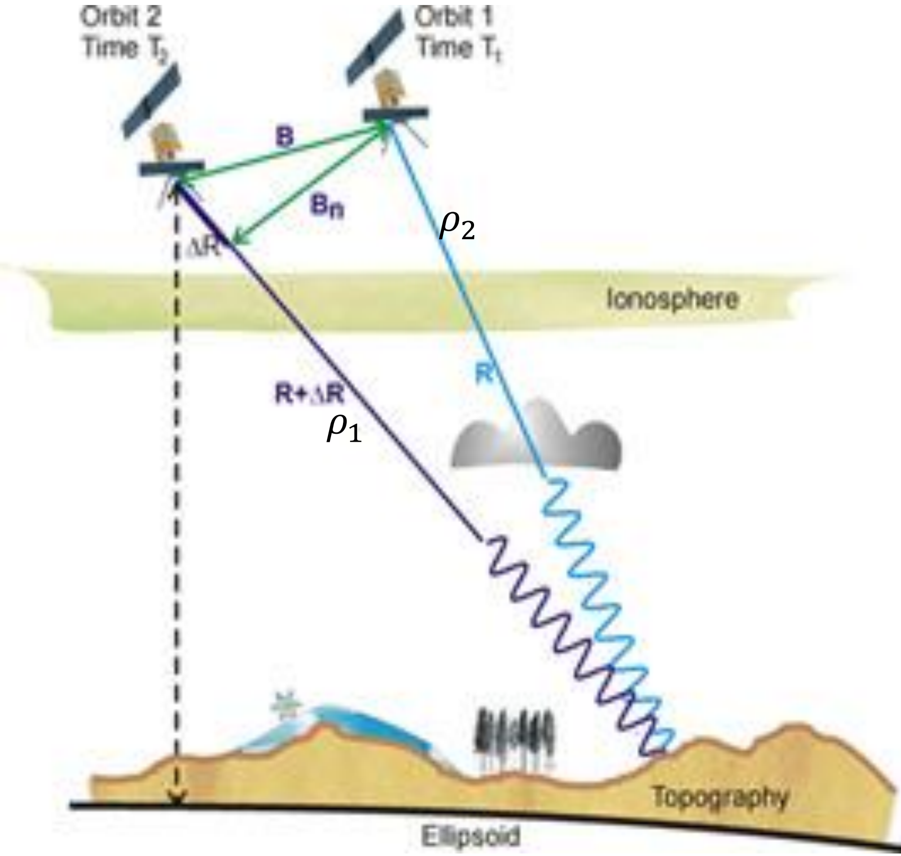

Radar Scattering Concepts I

- The measured radar backscatter signal in a focused 2D image is the complex sum of contributions from all elemental scatterers within each resolution element (pixel or "resel")
- These contributions add together as vectors in a random walk with the angle of each vector distributed uniformly over the primary interval (−π,π) where the p_k are the distances from the radar to each of the scatterers within the resolution element having center coordinates r and x and λ is the radar signal wavelength.

$$z_{r,x} = \frac{1}{\sqrt{N}} \sum_{k=1}^{N} a_k e^{\frac{-j4\pi\rho_k}{\lambda}}$$

$$z_{r,x} = e^{\frac{-j4\pi r}{\lambda}} A_{r,x} e^{j\phi_{r,x}}$$

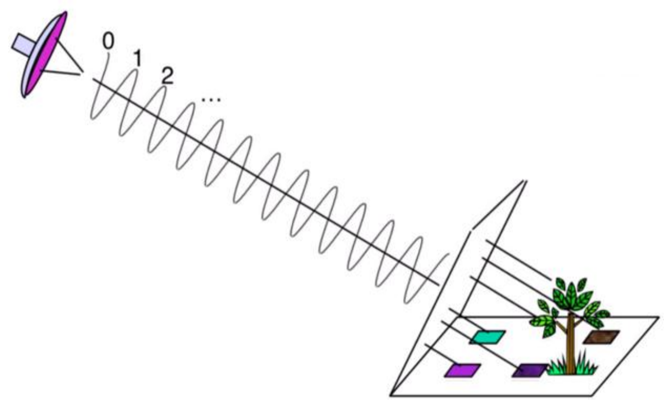

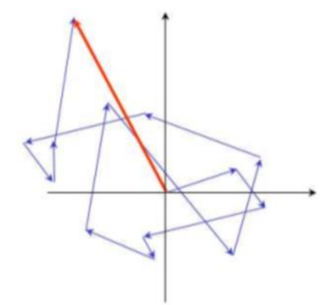

Blue: contribution by one single scattering event
Red: final amplitude and phase of received signal

Topographic Mapping Missions: TanDEM-X X-Band

	Spatial Resolution	Absolute Vertical Accuracy (90%)	Relative Vertical Accuracy (point-to-point in 1° cell, 90%)
DTED-1	90 m x 90 m	< 30 m	< 20 m
DTED-2	30 m x 30 m	< 18 m	< 12 m
TanDEM-X	12 m x 12 m	< 10 m	< 2 m
Level-4	6 m x 6 m	< 5 m	< 0.8 m

Visualization of improved DEM quality:

TanDEM-X vs. SRTM DEMs

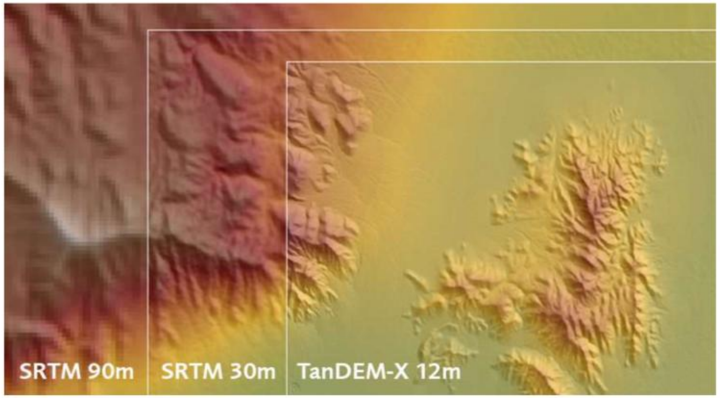

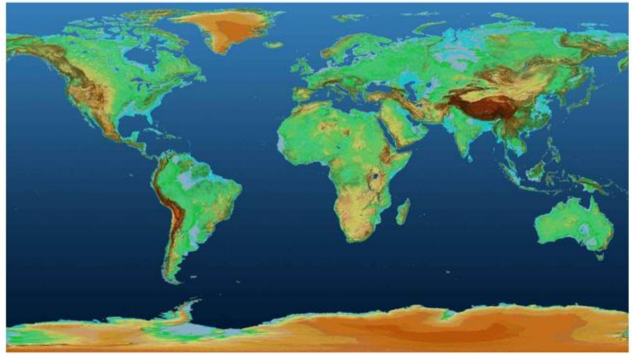

Deformation Mapping with Repeat-Pass Radar Interferometry

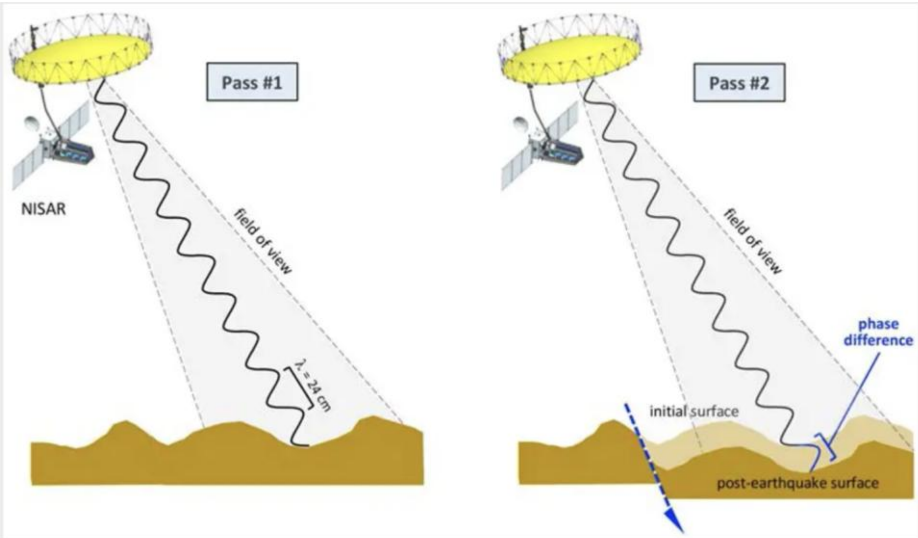

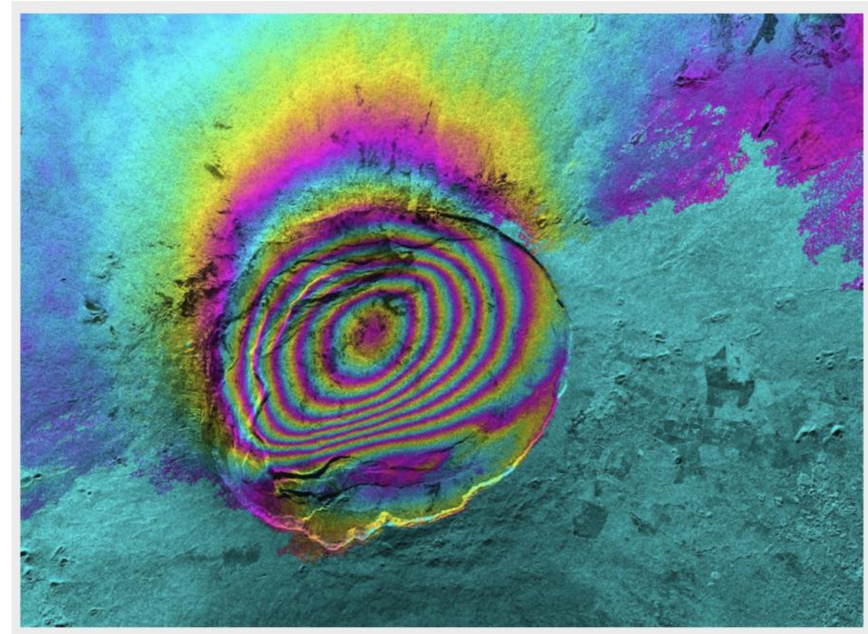

Measurement of the phase of the returned echoes permits high resolution imaging and the ability to map deformation at a fraction of the wavelength $\lambda = {}^{c}/_{f}$ where c is the speed of light, and f is the radar frequency

Interferometric Processing Workflow

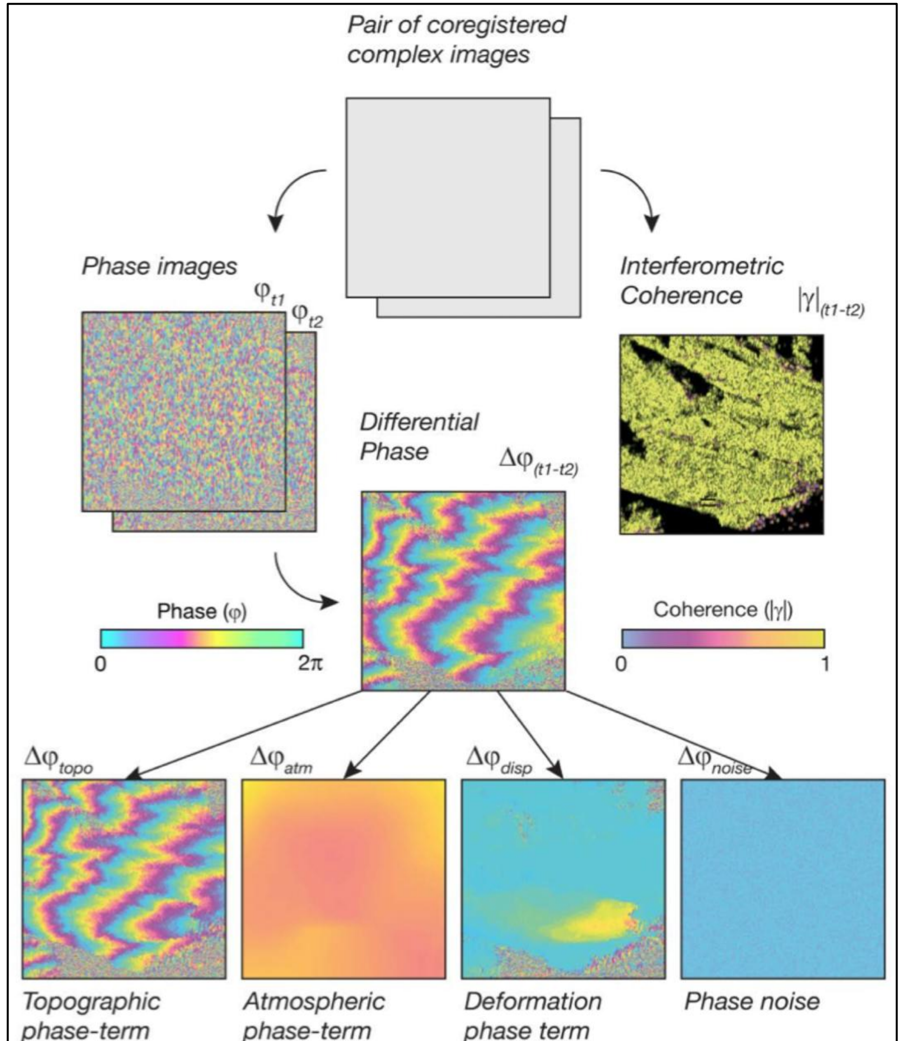

Applications of Radar Interferometry

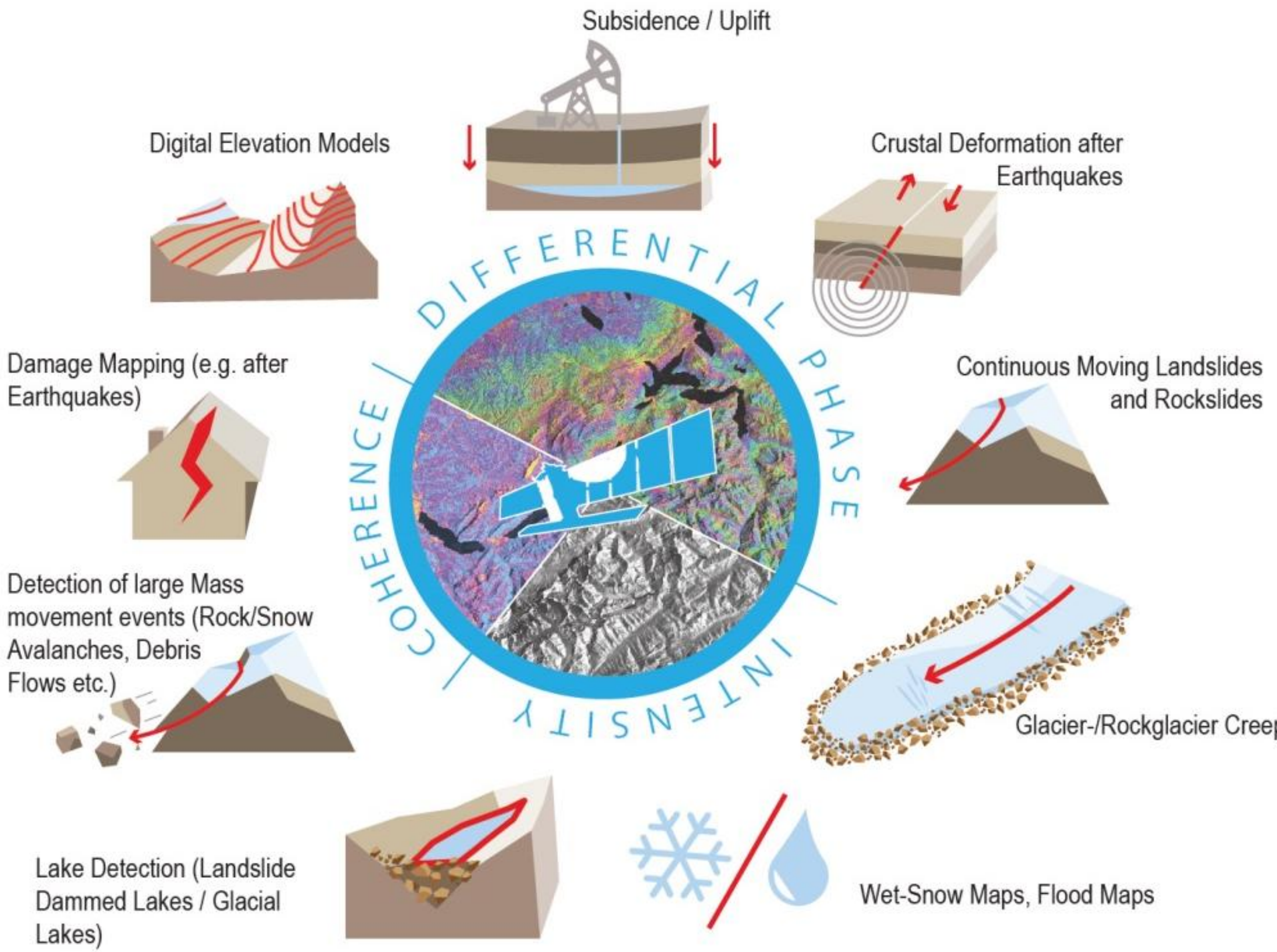

Interferogram and Coherence Map Calculation II

- Hector Mine earthquake 16-October 1999
- ERS-1, ERS-2 data acquired on 15-Sep-1999 and 20-Oct-1999

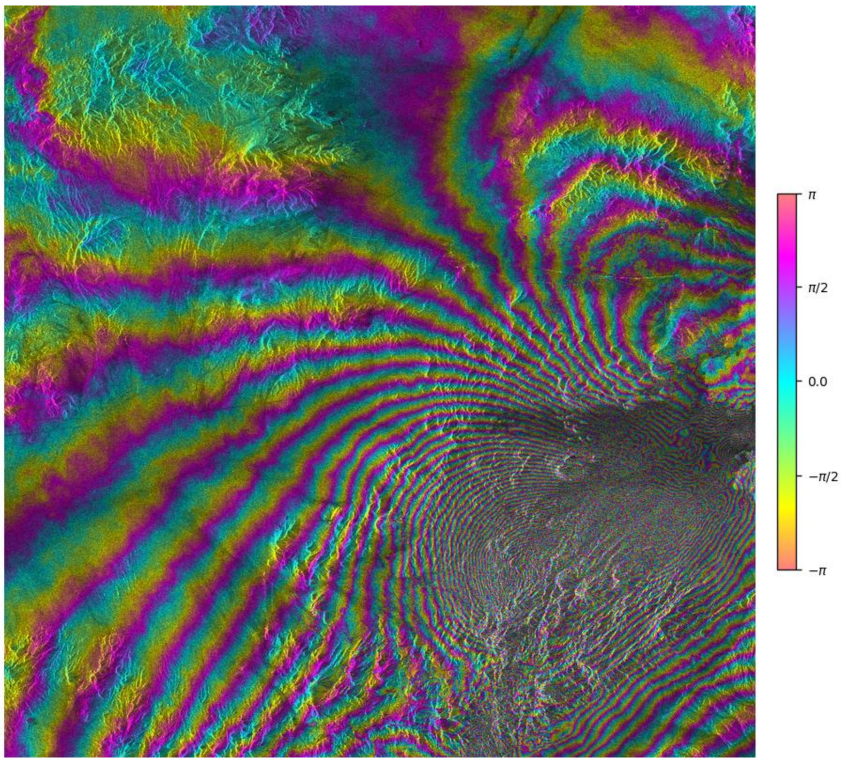

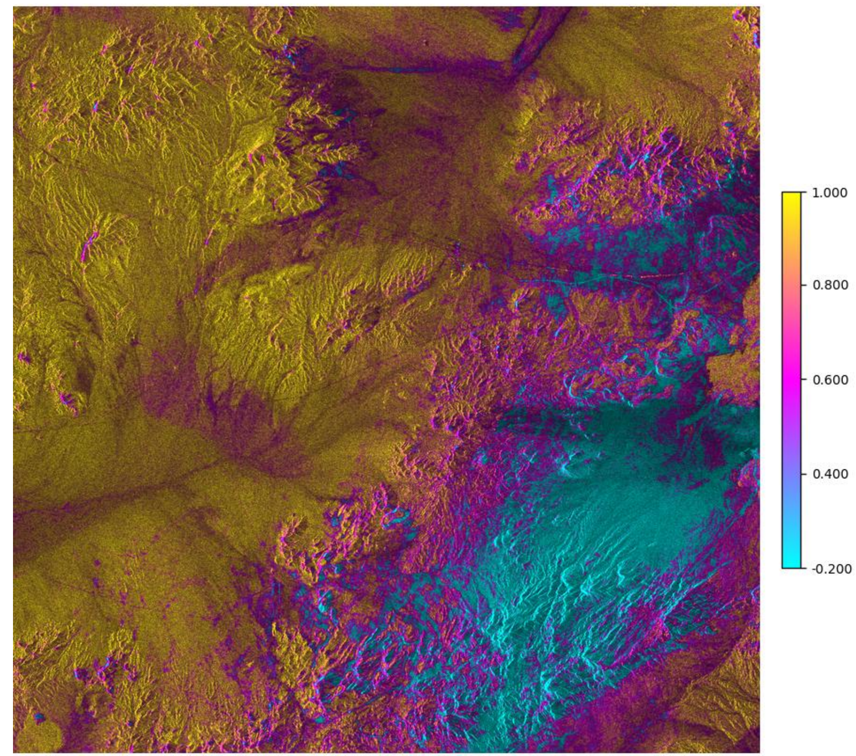

GAMMA REMOTE SENSING

Examples of INSAR Deformation Mapping

Interferograms in Support of Emergency Management

Example: 2023 M7.8 Turkey–Syria Earthquake

UNIVERSITY OF ALASKA FAIRBANKS

Modern SAR Sensors such as Sentinel-1 and the upcoming NISAR mission can provide InSAR data within 2-3 days of an event

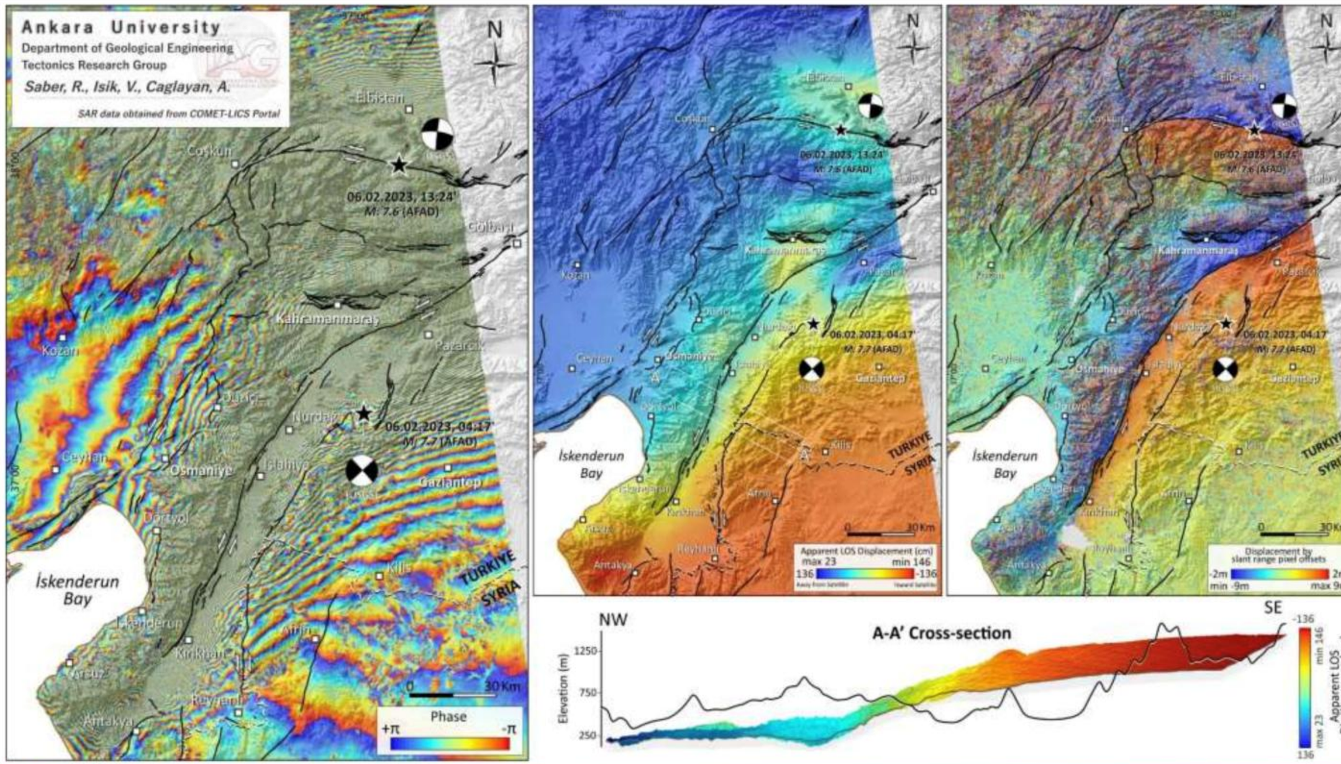

Franz J Meyer, UAF
GEOS 657 Microwave RS - 16

Ice Sheet Mapping

Continent-Wide Deformation Mapping from InSAR

Example: Antarctica

- First Antarctic-wide glacier velocity map in history
- Full coverage by merging data from a wide range of satellite systems
- Accuracy varies with number of multiple coverage per area and coherence

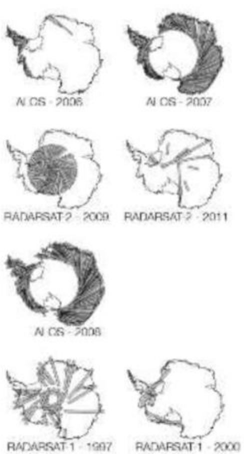

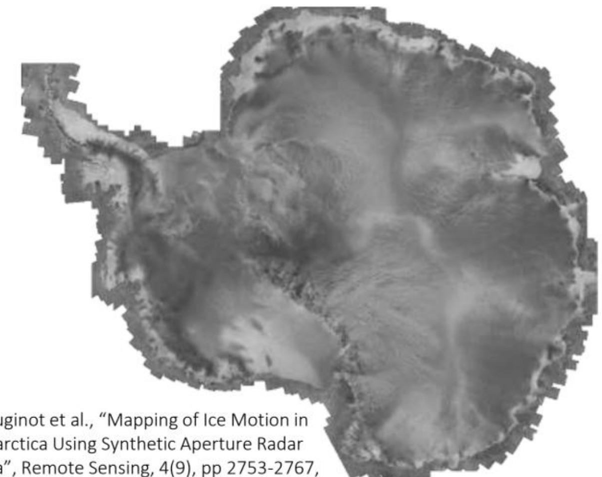

Mouginot et al., “Mapping of Ice Motion in Antarctica Using Synthetic Aperture Radar Data”, Remote Sensing, 4(9), pp 2753-2767, 2012

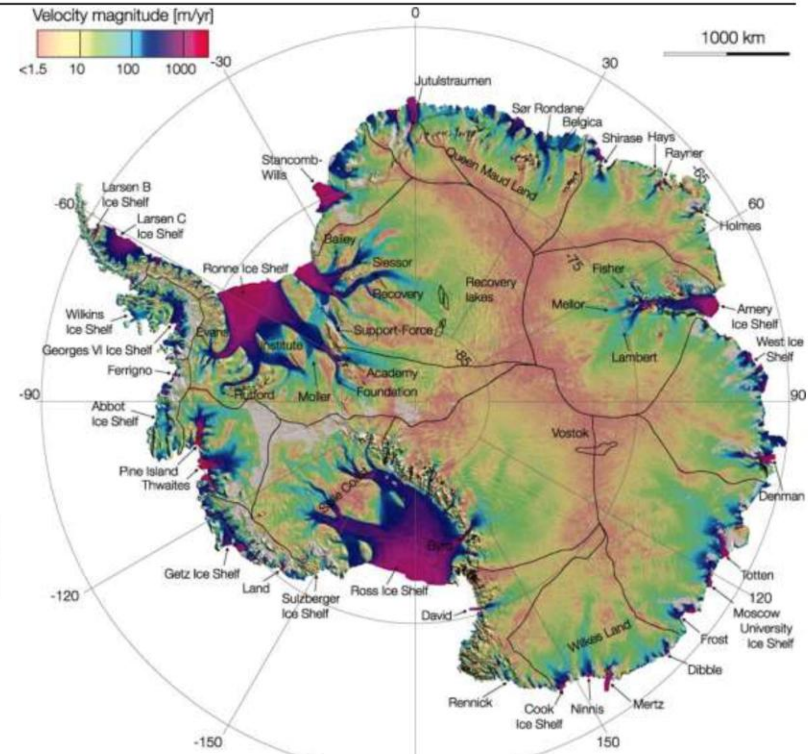

Courtesy: B. Scheuchl, UC Irvine

Volcanic Inflation in Alaska

Interferometric Phase Interpretation

Example: Surface Deformation at Mt. Peulik, Alaska

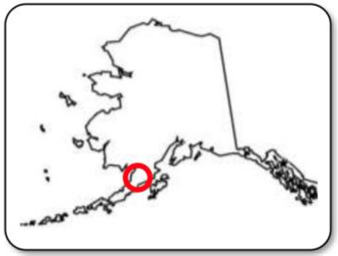

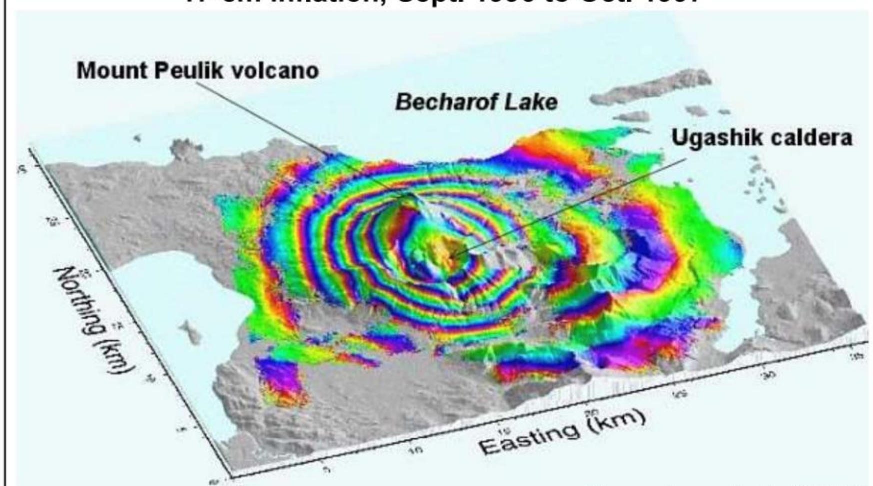

Zhong Lu, et al. (2001)

Challenges for Deformation Measurement with DInSAR

1. Variable atmospheric propagation delays
   a. Independent of frequency
2. Variable ionospheric propagation phase and attenuation (orbital instruments)
   a. Ionosphere phase results defocusing and image shifts: f^{-2} frequency dependence
      - Loss of accuracy for deformation, coregistration errors → lower coherence
   b. Polarimetric distortion
3. Temporal decorrelation: frequency dependent
4. Insufficient sampling rate for rapid deformation
   a. Temporal decorrelation introduces phase noise: frequency and surface dependent
5. Lack of angular diversity leads to coverage loss from layover/shadow
6. Insufficiently long measurement time-series for slow deformation
7. Insufficient spatial resolution for localized hazards (rock falls, landslides)

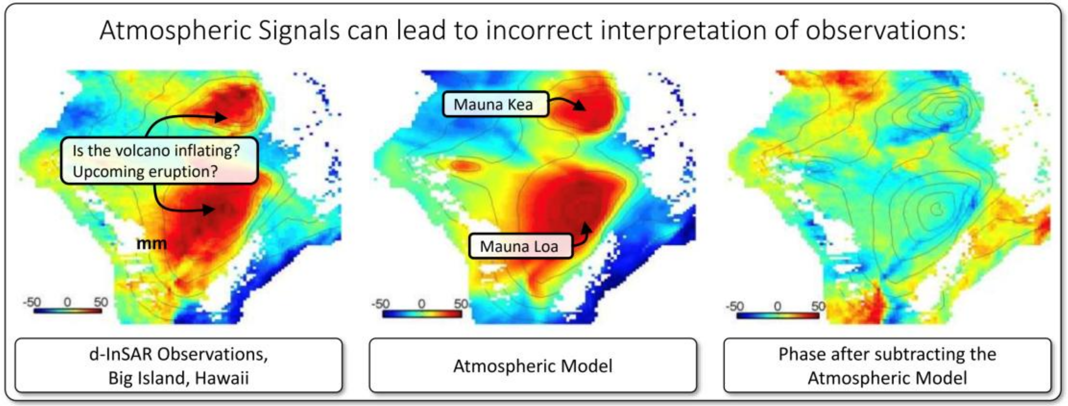

Gornergletscher, Valais

30-Sep-2005

Gamma Portable Radar Interferometer

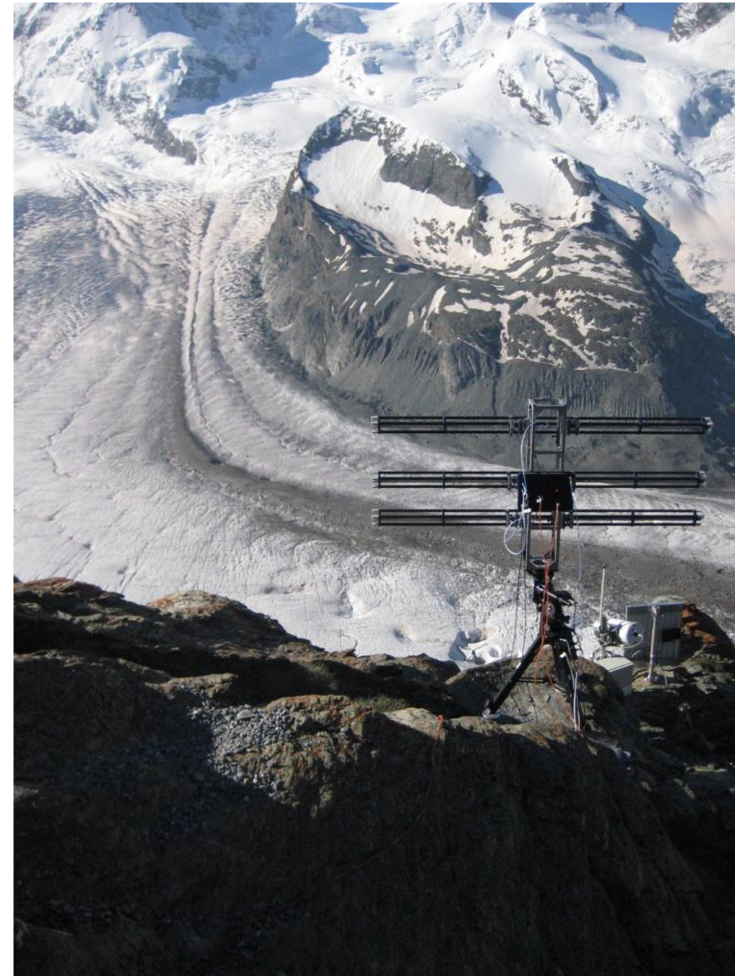

23-Jun-2008

Gorner, Grenz and Zwillings Glaciers

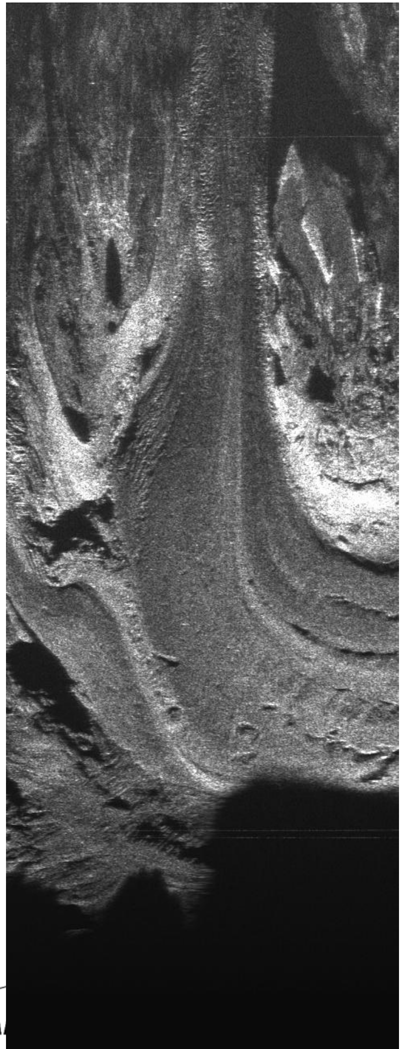

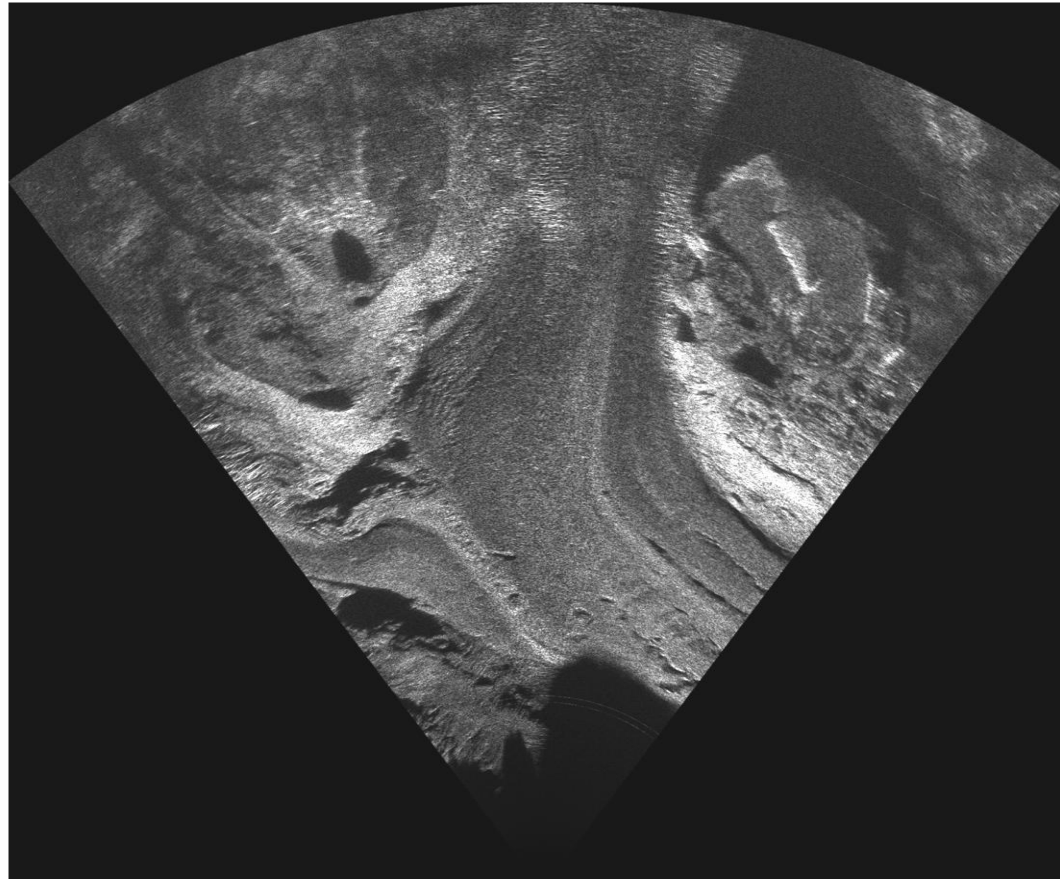

Range out to 4.5 km from observation point

Gorner, Grenz and Zwillings Glaciers

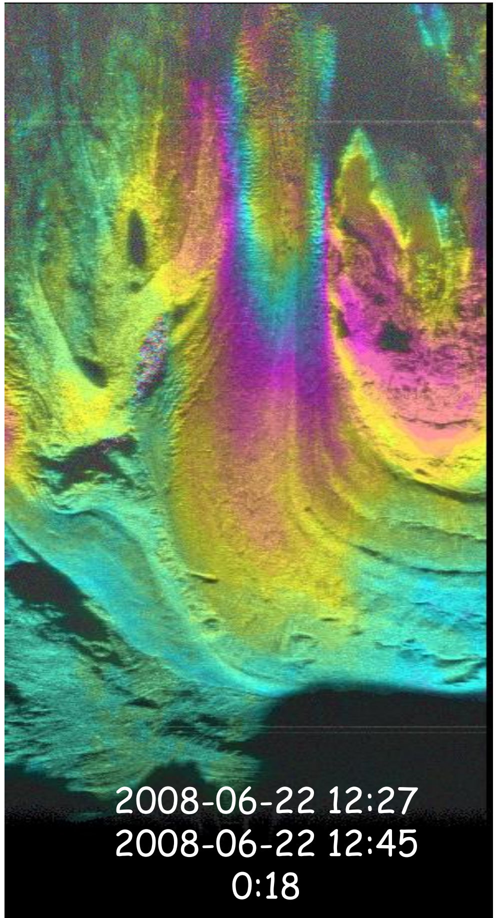

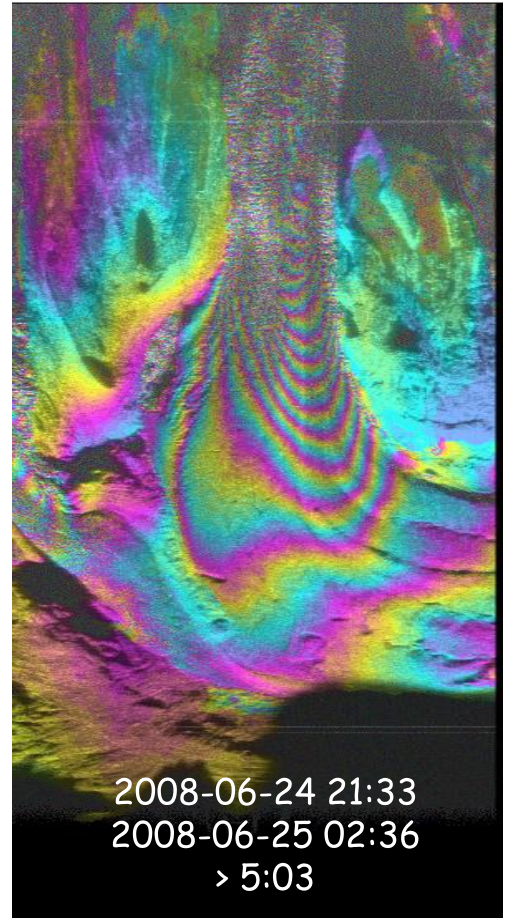

$2\pi \Leftrightarrow$ 8.72 mm @ 17.2GHz

GPRI-II Instrument Characteristics

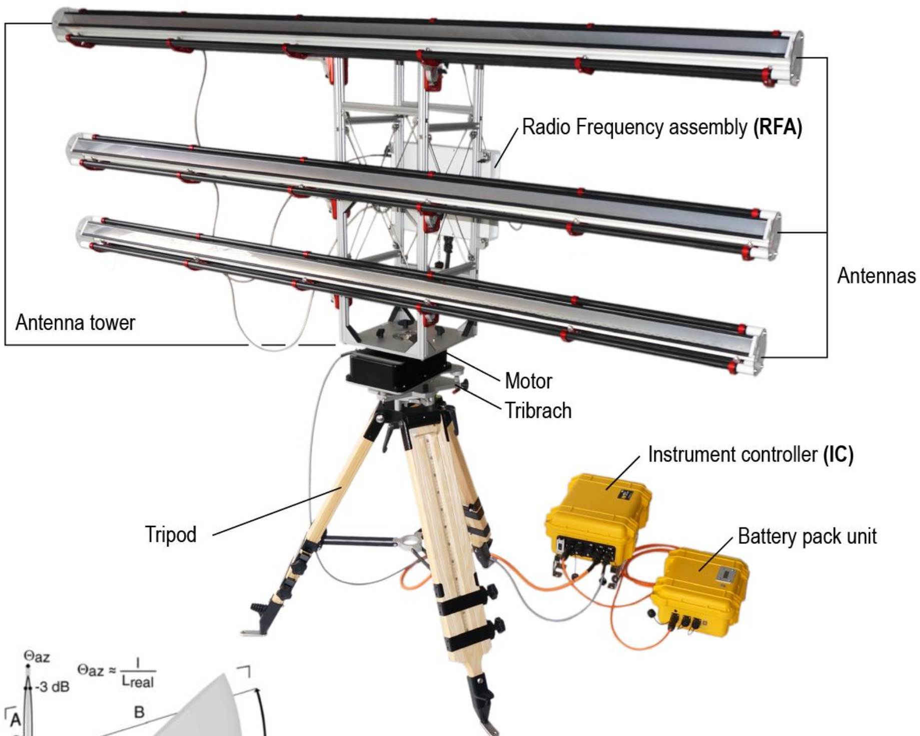

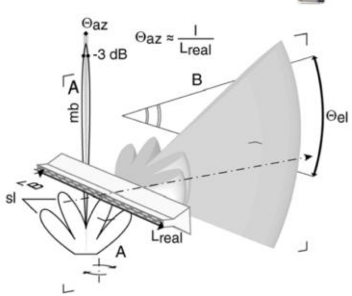

- Frequency: 17.2 GHz, wavelength: 17.43 mm
- Antennas: 2m slotted waveguide
- Beamwidth 40 deg Elev., 0.385 deg Az.
- FCC Approved
- 50 kg, fits in a pickup or SUV
- Tripod or monument mount
- Transmitter power: 250 mW
- Radar Type: FMCW
- 2 Independent receivers permit DEM measurement and redundancy
- Resolution: 0.9m range, 6.85 m @ 1km Azim.
- Power: 35-80 W, Li-ion Battery pack: ~ 4hrs operation
- Computer: Intel Core i5, 1 TB SSD, Ubuntu Linux 20.04
- Python software for data acquisition and control with GUI for data acquisition and data quality assurance
- Python scripts for terrain geocoding, interferogram generation
- Gamma Software for interferometric processing and display. Python scriptable.

GPRI-II Radar System Design

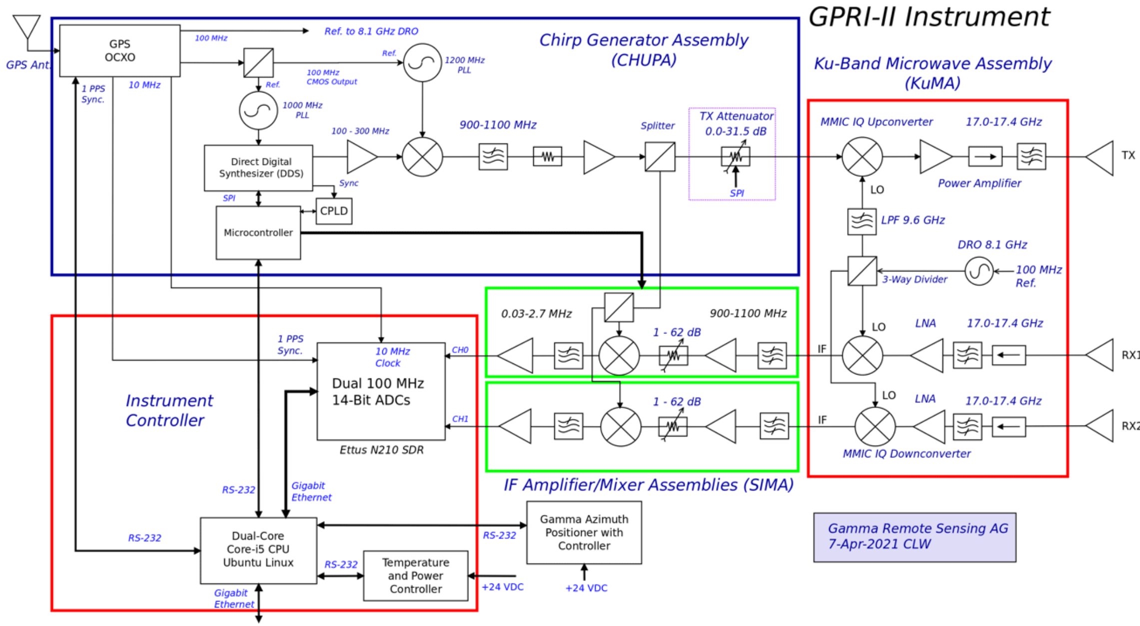

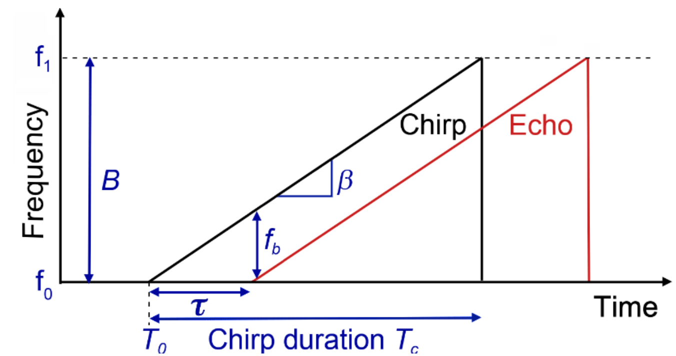

$$R_{max} \approx \frac{c f_s T_c}{4B}$$

$$\delta_r \approx \frac{c}{2B}$$

- The GPRI is a dual channel FMCW radar
- Direct Digital Synthesis (DDS) of the chirp
- Uses a dual-channel Software Defined Radio (SDR) to digitize the deramped signal
- Linux PC for instrument control and data logging

GPRI Observation Modes

1. Continuous : deformation measurement mm to m/day
2. Revisit: mm to cm/year
3. Staring: rapid deformation of a bridge or building
4. Topography: measurement of height or height change
5. Slow-Scan: wave and current measurement

Mine Slope Stability: Fairview Pit Round Mountain, Nevada

- Continuous Mode: GPRI-II Installation on total station mount
- Distance ~500 meters
- 450 observations at 2-minute intervals 20130708_214031 → 20130710_204112
- Slope failure clearly delineated, what is the risk?

Fairview Deformation Time-Series 9-10 July 2013

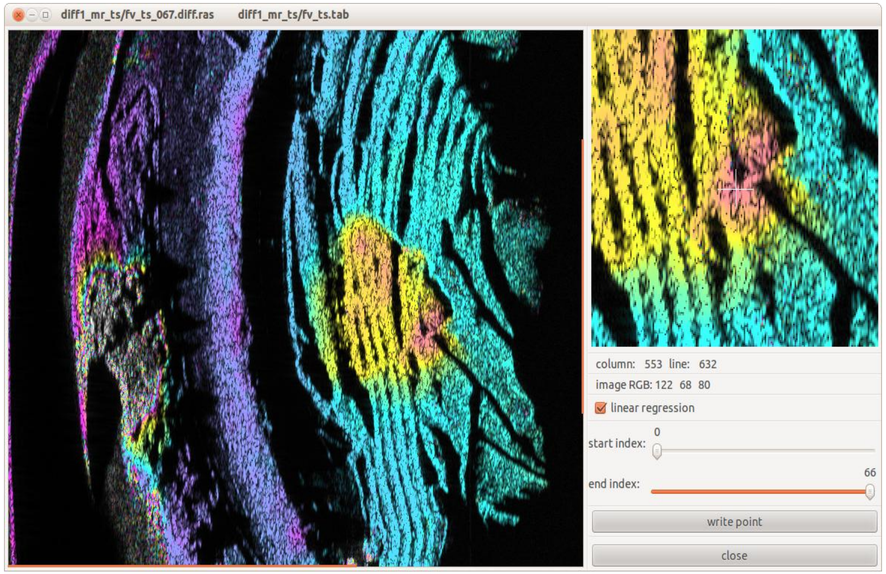

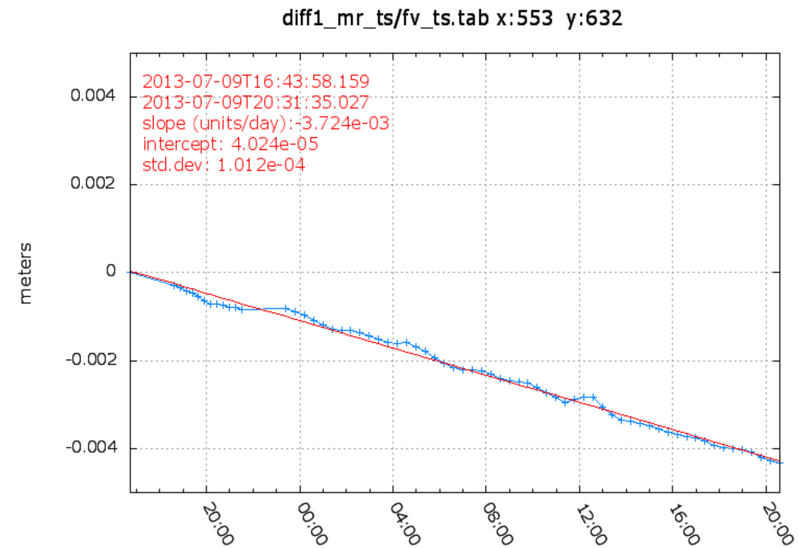

- Time-series solution using GPRI2 data
- Temporal smoothing applied to reduce variations in atmospheric time delay

Round-Mountain Gold Mine, Nevada 2017

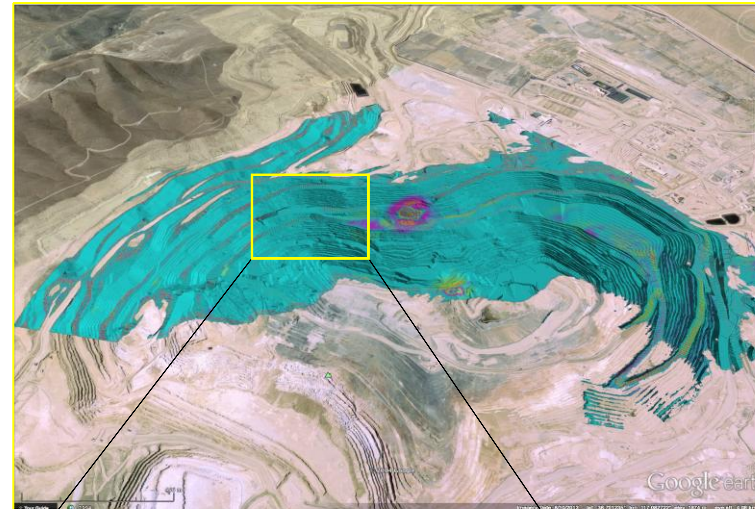

- Slope deformation over 1 day, each fringe represents 8 mm line of sight (LOS) motion.
- Trailer mount with leveling for deployment at a without concrete base
- Radome provides long-term environmental protection from wind and UV.

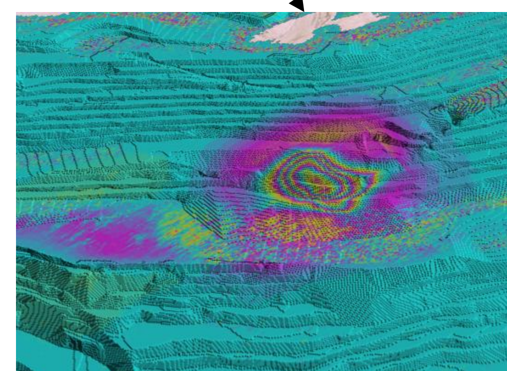

GPRI-II Instrument at Brinzauls, Switzerland

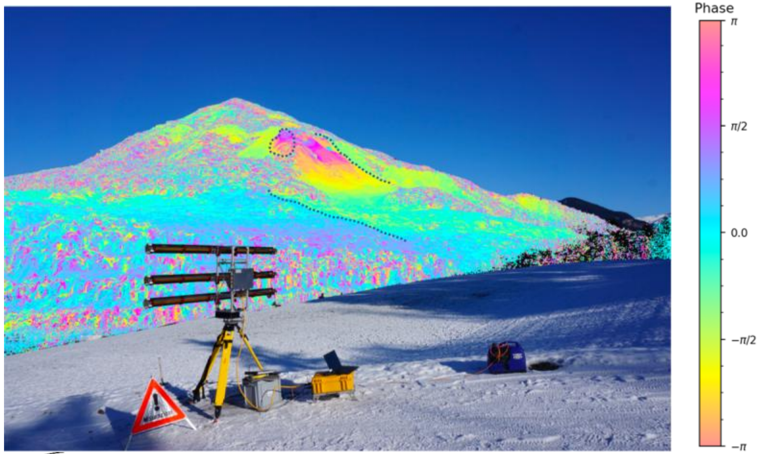

- Brinzauls landslide near Davos Switzerland
- GPRI-II measurement: 10:46 and 18:19 22-Jan-2020
- One color cycle is equivalent to 8.72 mm

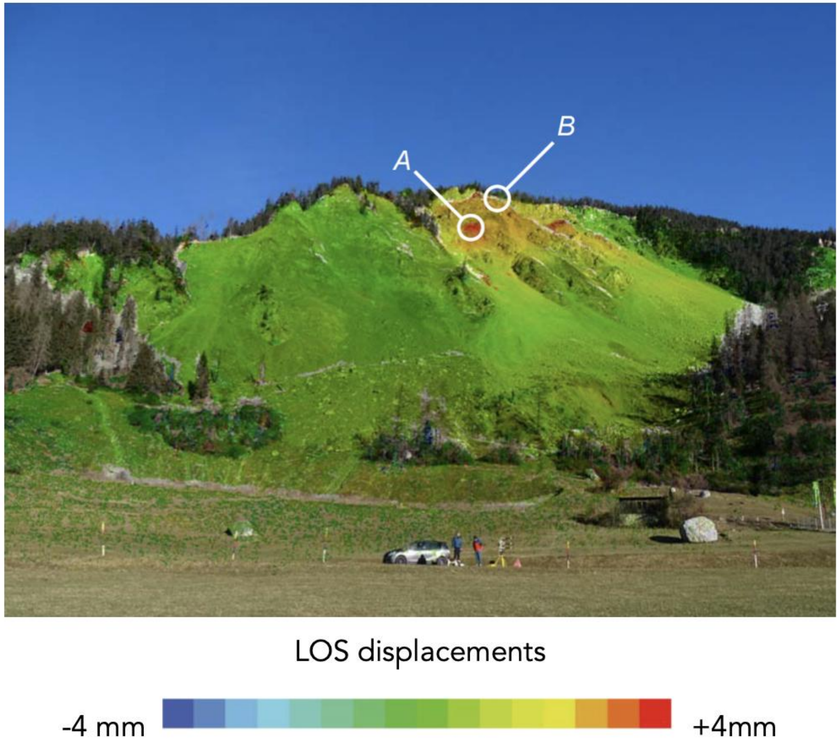

GPRI-II Radar at Oroville Dam, California

GPRI-II Radar at Oroville Dam, California (Sept. 2020)

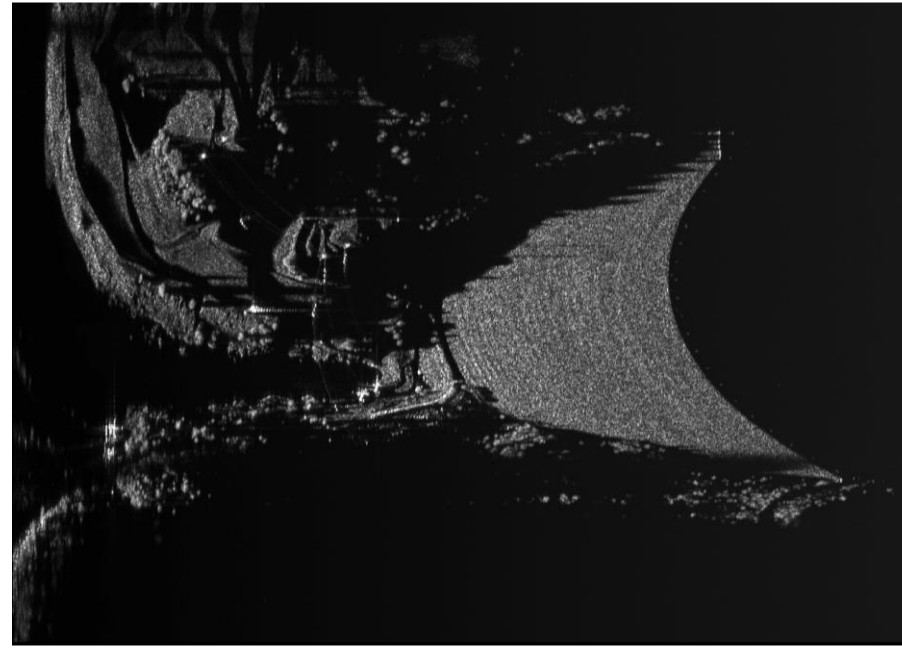

- The GPRI-II is a 17.2 GHz ground-based real-aperture radar (RAR), wavelength 17.42 mm
- Operates by rotational scan of antennas with beamwidth 0.385x30 degrees
- Scan repeat interval: 60 seconds

GPRI-II Radar at Oroville Dam, California, USA

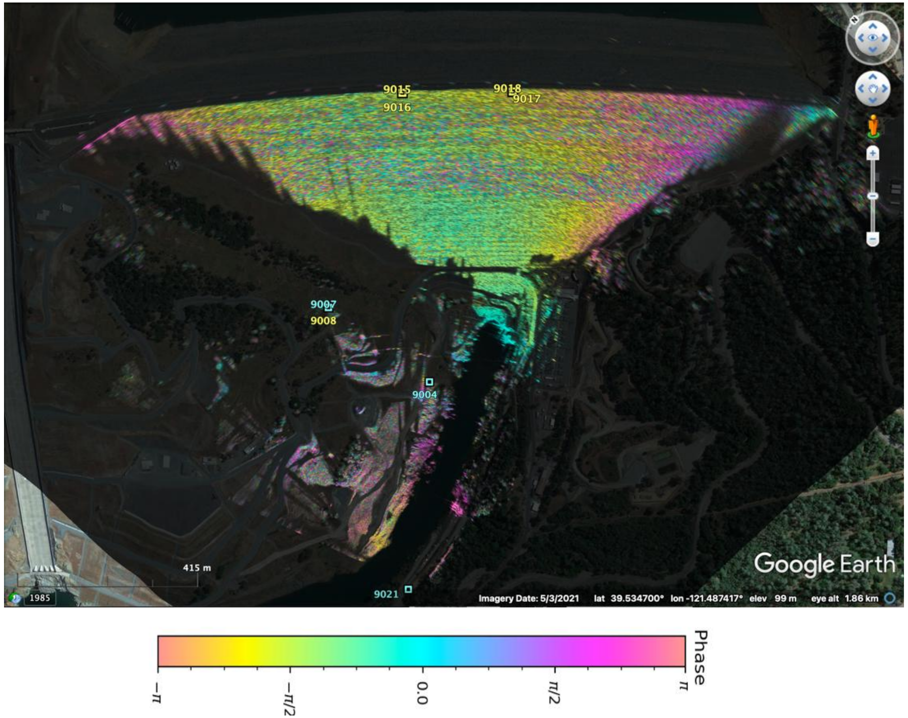

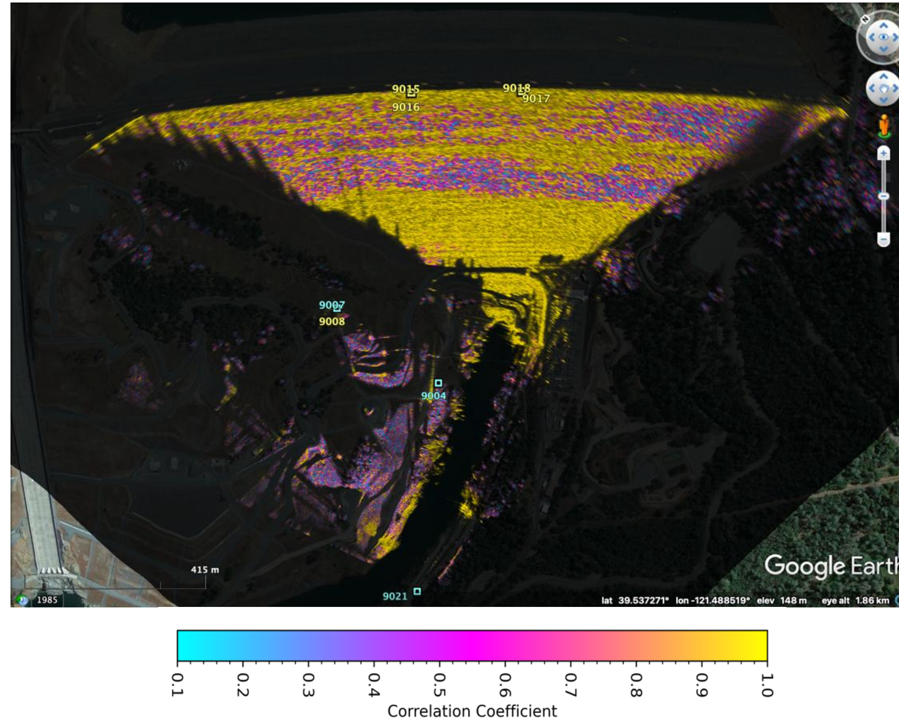

- Geocoded differential interferometric phase combined with radar backscatter intensity for the Oroville dam (left), and interferometric correlation (right).
- Images acquired on 20210108 and 20210120 from the Alpha Site

CarSAR GSL and GLSAR Measurements at Brinzauls, Switzerland

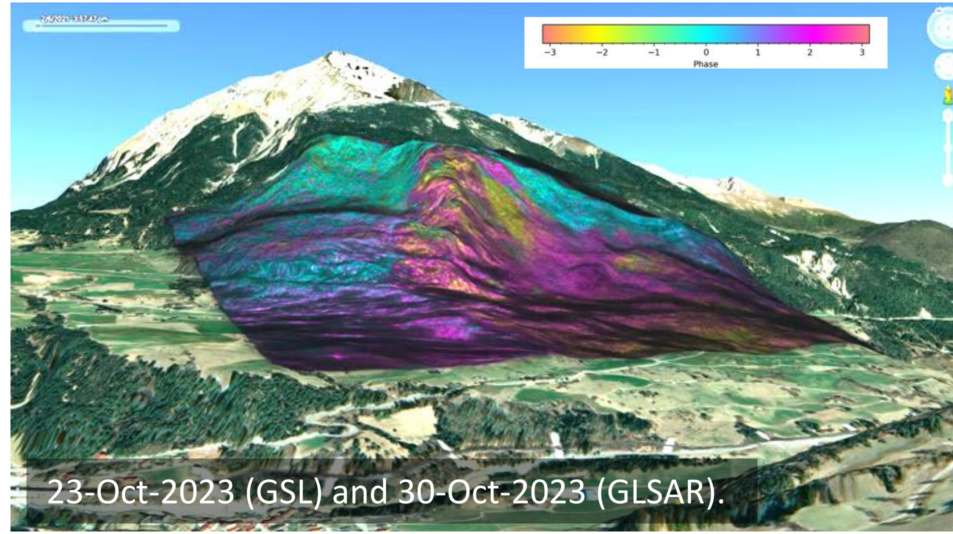

- The Gamma L-Band SAR (GSL) was developed in 2017 for UAV and CarSAR imaging
- This FMCW radar operates with a bandwidth up to 200 MHz, 1.2-1.4 GHz
- The Brinzauls landslide was moving cm/day after a large event
- 2π phase is equivalent to 11.31 cm of deformation long the line of sight

CarSAR GSL and GLSAR Measurements at Brinzauls, Switzerland

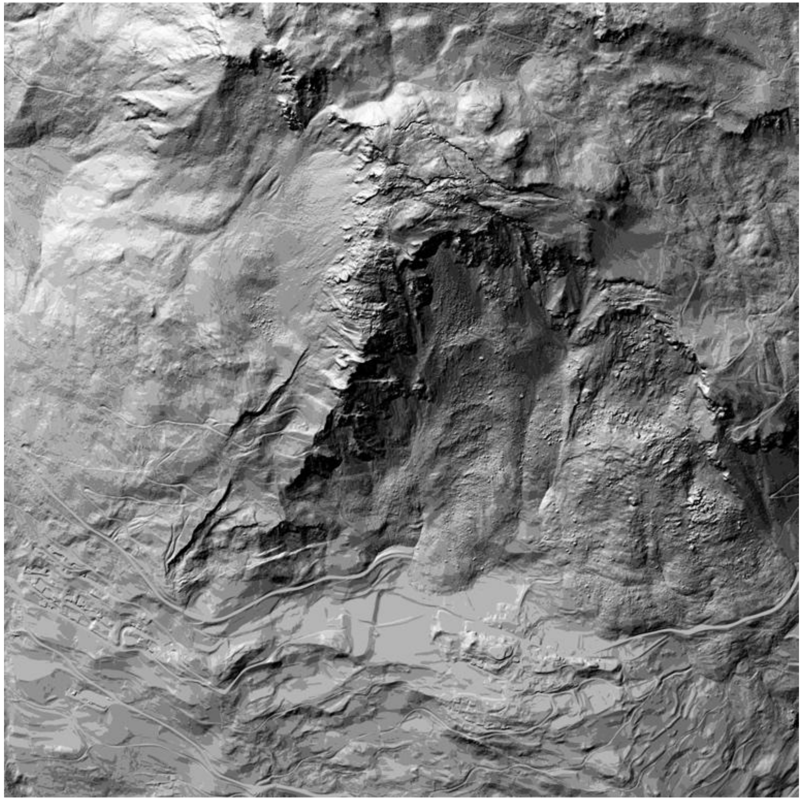

Shaded relief from DEM, 2 km x 2 km region

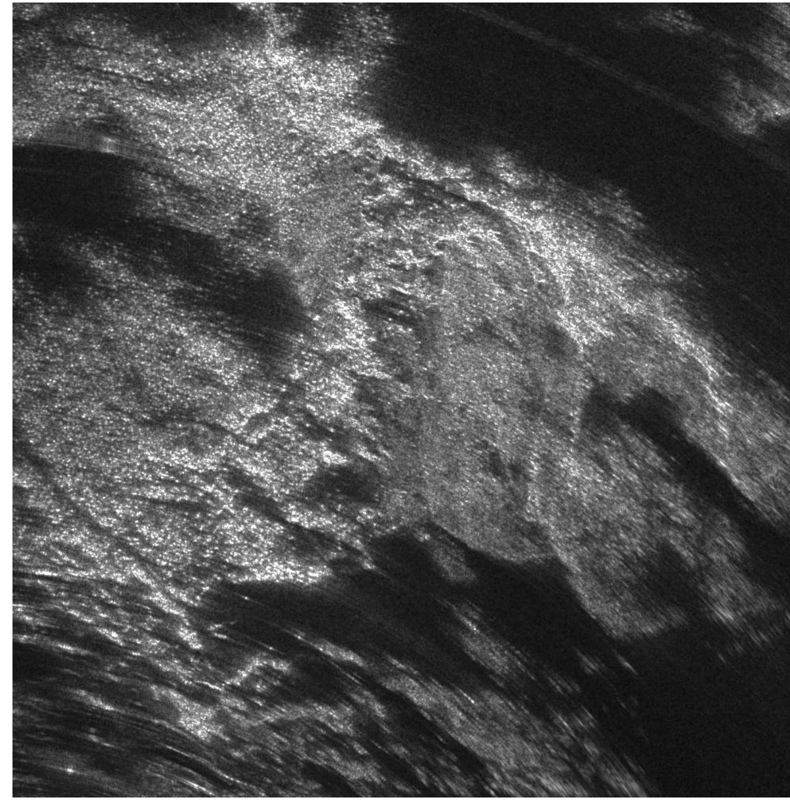

GLSAR multi-look intensity image The radar operated with 100 MHz bandwidth 1275-1375 MHz

CarSAR GSL and GLSAR Measurements at Brinzauls, Switzerland

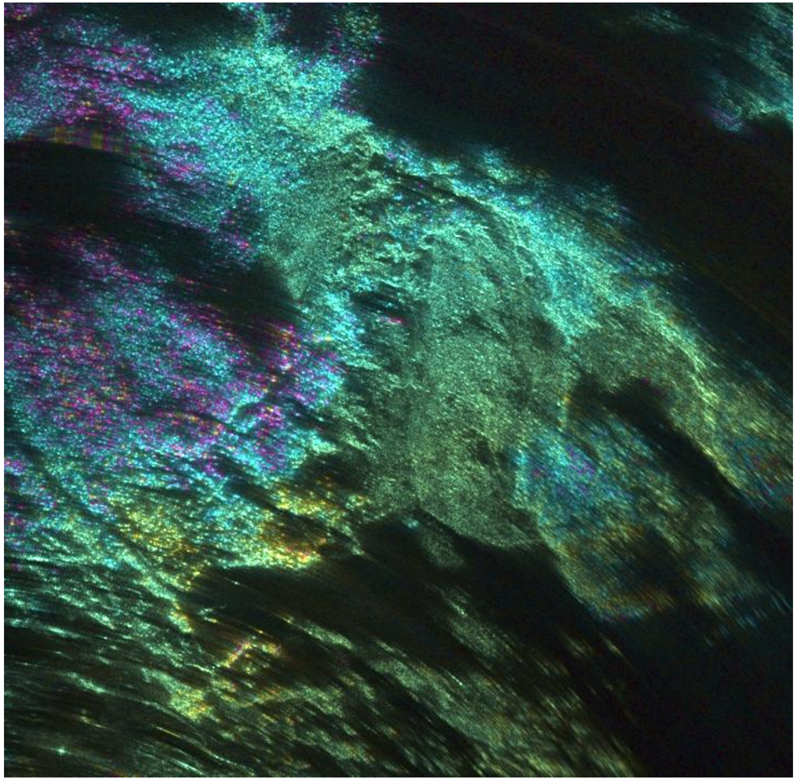

Differential interferogram with 14-minute time interval acquired with the GLSAR on 30-Oct-2023

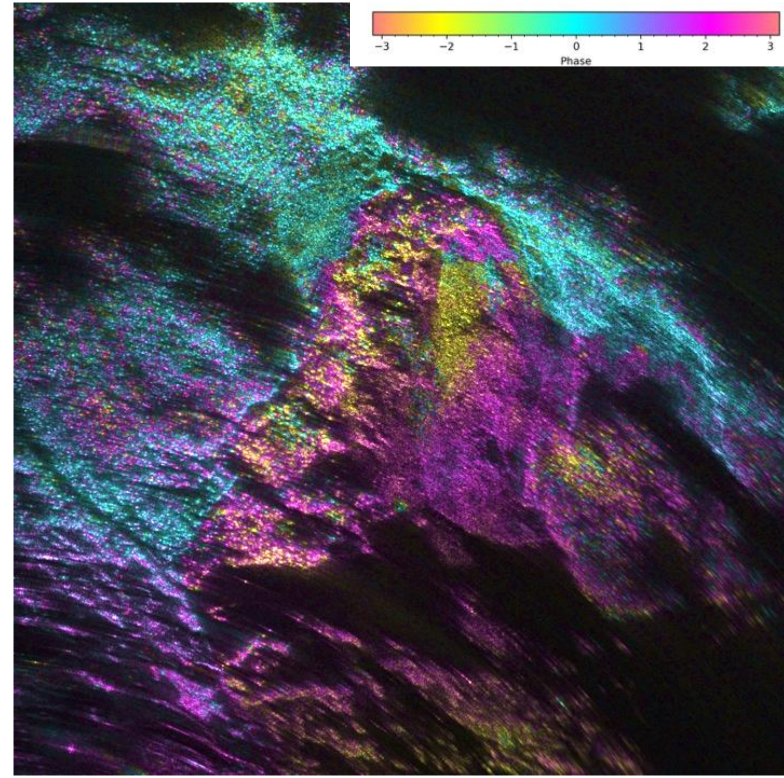

Differential interferogram 23-Oct-2023 (GSL) and 30-Oct-2023 (GLSAR). 2π phase is equivalent to 11.31 cm of deformation in the LOS

Gamma GLSAR L-Band Radar: 1.2-1.4 GHz

Frequency Range	1.2 to 1.4 GHz
Range resolution	1.0 meter @150 MHz bandwidth
Azimuth Resolution	0.3 meters
Transmitter Power	Programmable up to 10 Watts
Number of Transmit Channels	2
Number of Receiver Channels	4
Analog to Digital Converter Bits/Sample	14 bits
Data Sampling Modes	Offset Video/Quadrature (IQ)
Antenna 3 dB Beamwidth	49 degrees x 49 degrees
Antenna Polarization and Gain	12 dB gain, H, V polarization
Radar Electronics Dimensions and Mass	25.8 x 25.8 x 10 cm, 3.9 kg
DC Power Input	32 to 54 VDC < 3A, < 120W
Antenna Frame + Antennas	2.5 kg
Onboard Data Storage	2 TB
I/O Interfaces	Gigabit Ethernet, USB3
Environmental	IP 64, Temperature: -35 to +45 C

Gamma GSSAR S-Band Radar: 3.0-3.4 GHz

System Parameter	GSSAR
Frequency Range	3.0-3.4GHz
Slant Range Resolution	45 cm @400 MHz BW
Azimuth Resolution	0.3 meters
Transmitter Output Power	Programmable up to 8W
Number of Transmit and Receive Channels	2 Transmit, 4 Receive
Analog to Digital Convertor Bits	8-16@100 MHz sampling rate
Decimation factors supported by the DAS	1,2,4,6,8,12,16,20
Maximum data transfer rate to SSD	68 Mbytes/s
Antenna 3 dB Beamwidth	30 deg. Elev., 17 deg. Azimuth
Antenna Polarization and Gain	16 dB gain, H, V polarization
Noise Equivalent Sigma0 @1km Alt., 50 deg. look ang., 33 m/s velocity, TX Power: 4 W	-58 dB
Radar Electronics Mass and Volume	25.8 x 25.8 x 10 cm, 3.9 kg
Radar Dimensions and Mass with Ant. Frame	32 x 52 x 140 cm, 6.4 kg
DC Power Input	32 to 54 VDC, 120W Max.
Onboard SSD Data Storage	2 TB
I/O Interfaces	Gigabit Ethernet, USB3, Serial, GPIO
Environmental	IP 65, Temp.: -35 to +45 C

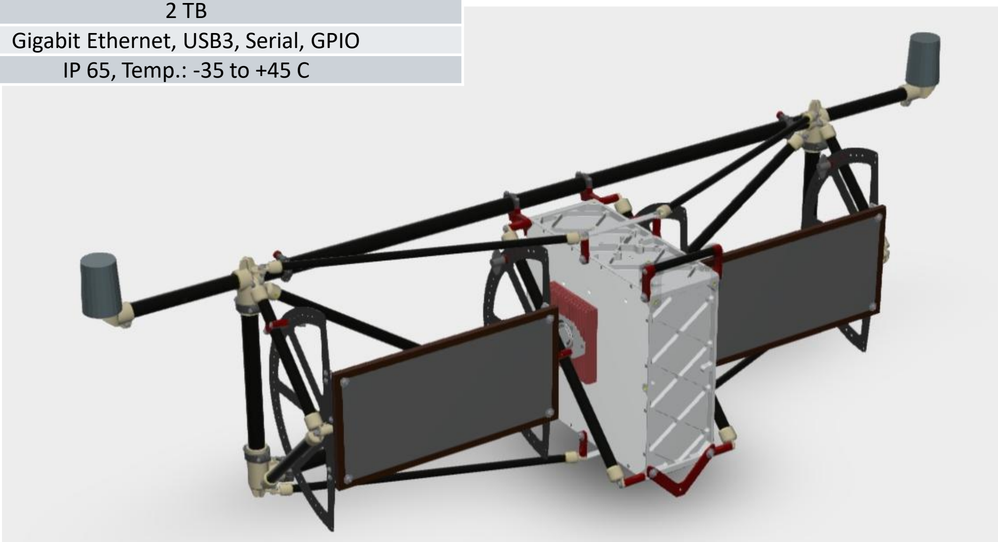

GxSAR Instrument for UAV and CarSAR

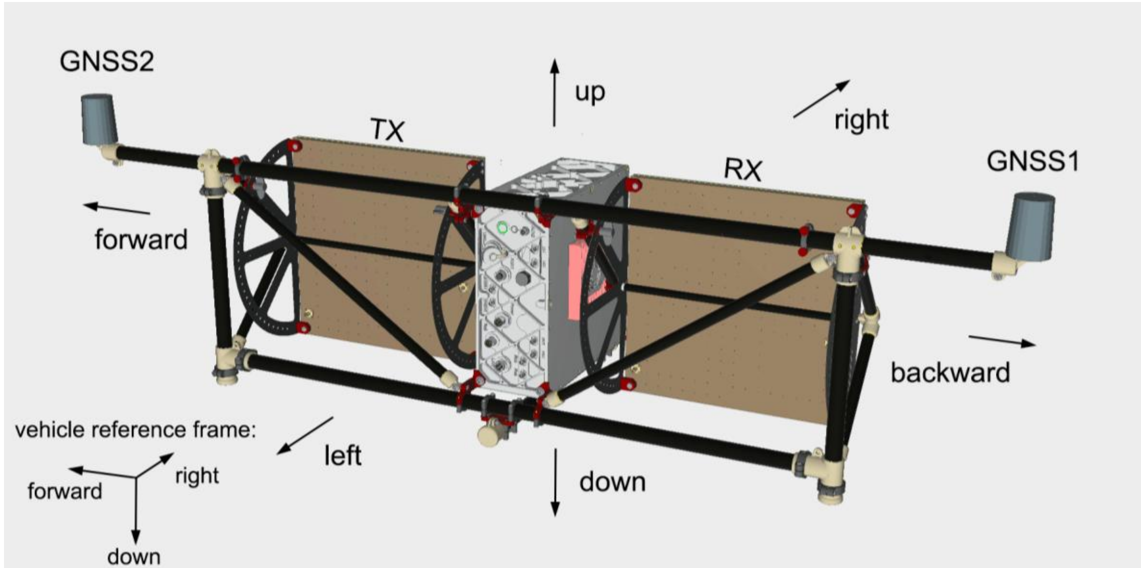

- Light-weight adjustable carbon tube frame
- Planar Microstrip broadband patch antennas. H, V input ports
- 4 Rx channels, Alternating TX1, TX2
- ~4.2 kg enclosure:
- Built-in INS (Honeywell n500 + NovAtel OEM7720 GNSS)
- Linux PC for data storage and instrument control

GLSAR and GSSAR FMCW Radar Architecture

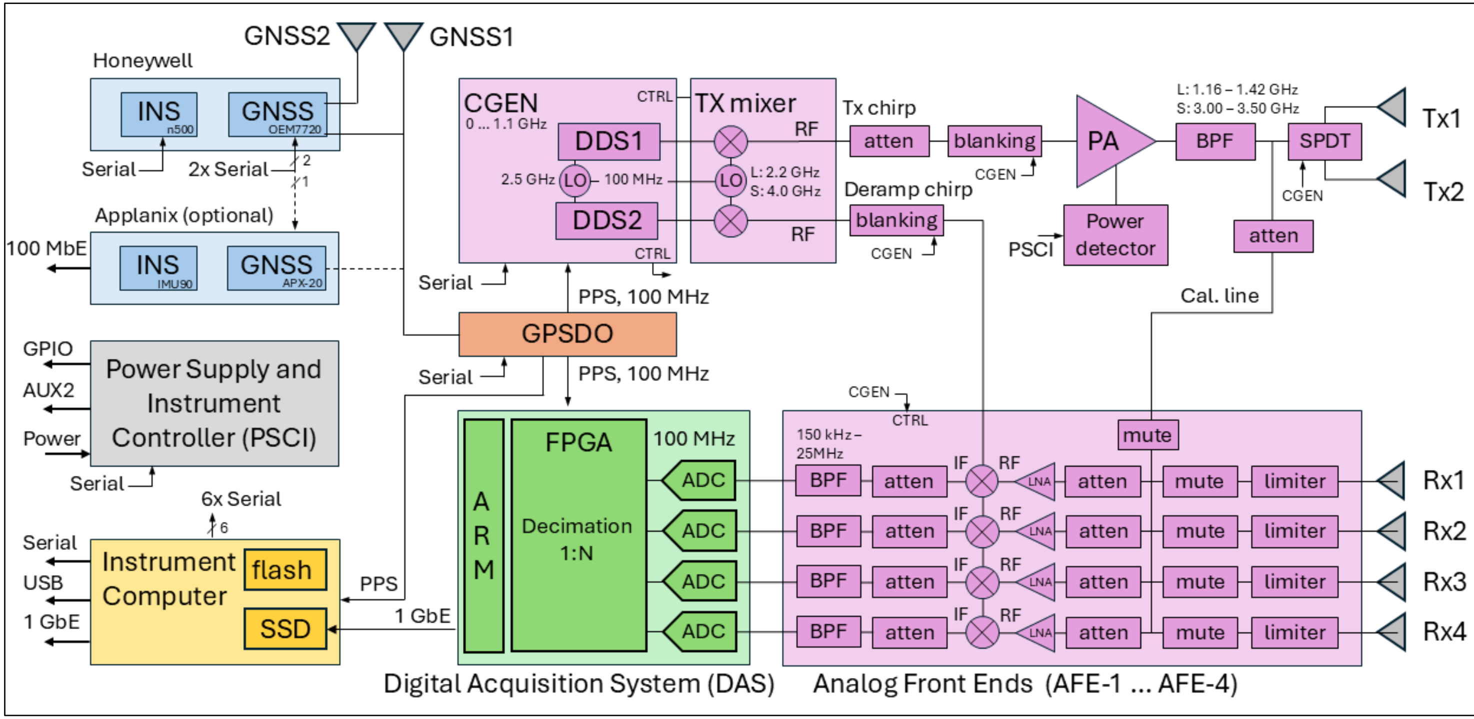

- Dual DDS chirp generation (BIT and Calibration)
- FPGA supports both Real-sampling and IQ-sampling modes (Swath-Tuning)
- TX and RX blanking (reduce transients)
- GPS disciplined oscillator for time and frequency reference
- Internal IMU/GNSS INS system (Honeywell n500 + NovAtel OEM 7720

GLSAR Electronics Assemblies

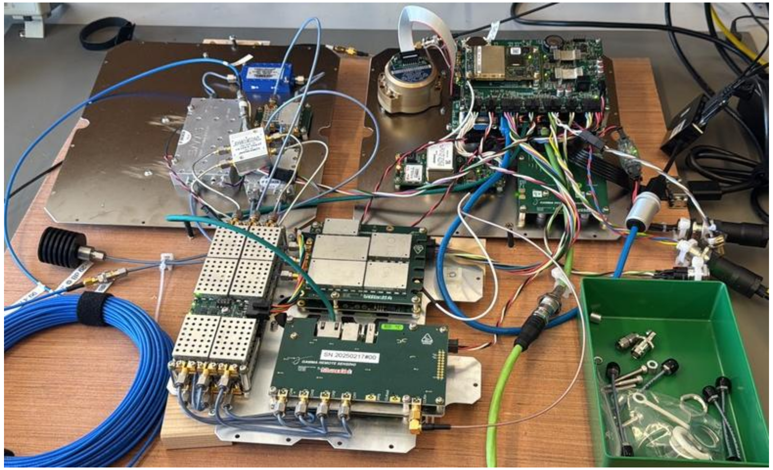

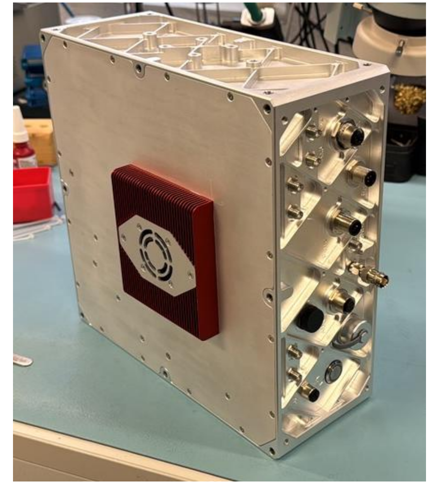

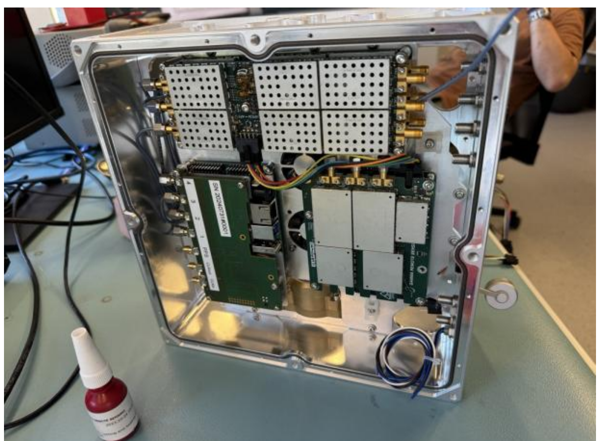

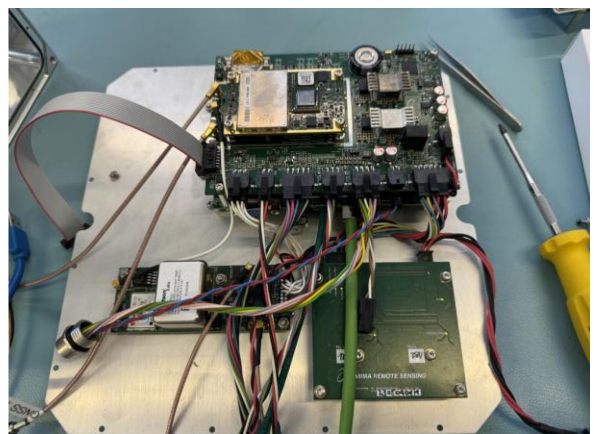

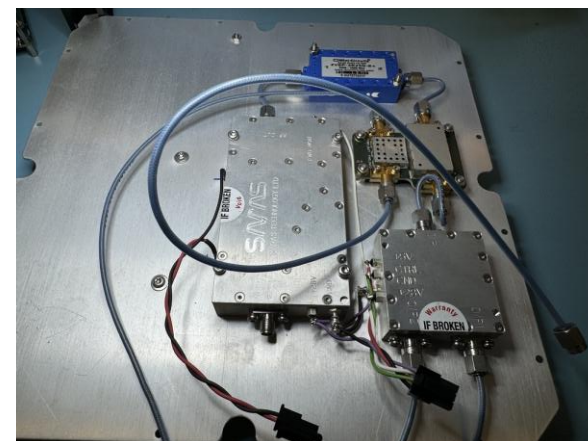

GSSAR Delay-Line Measurement

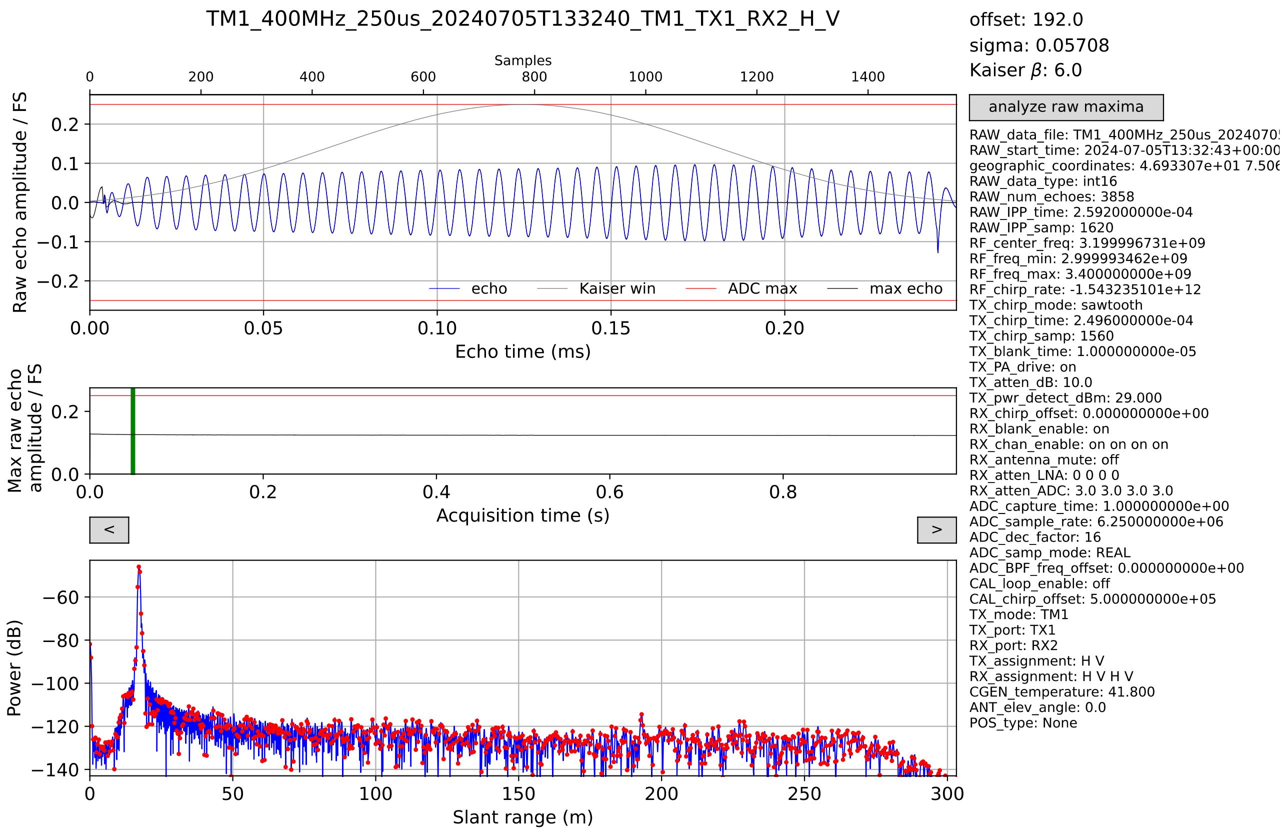

- Delay-line measurement
- 99 ns delay
- 80 dB spurious free dynamic range

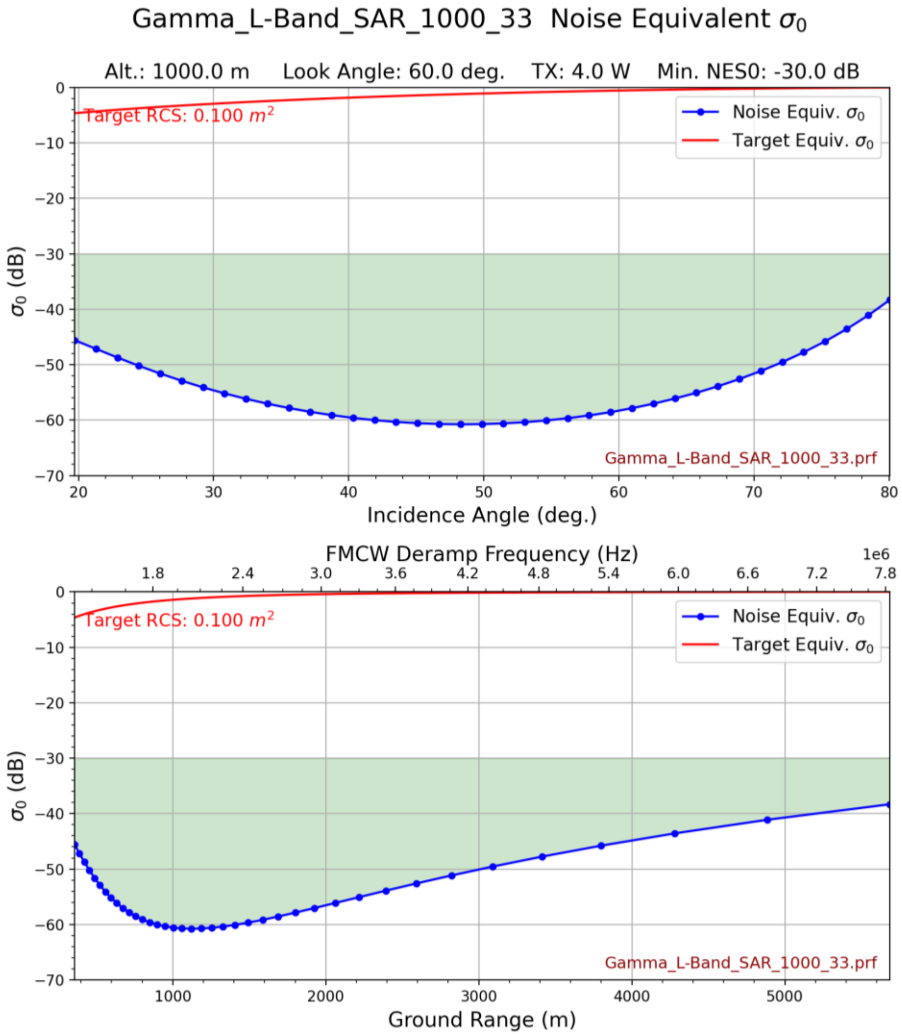

- Better that -50 dB NES0 across the swath 25→ 70 deg. look angle, 60 deg. boresight
- 1000 m altitude, long-track 120 km/h velocity (33.3 m/s)
- 4-Watt TX power, 200 MHz bandwidth

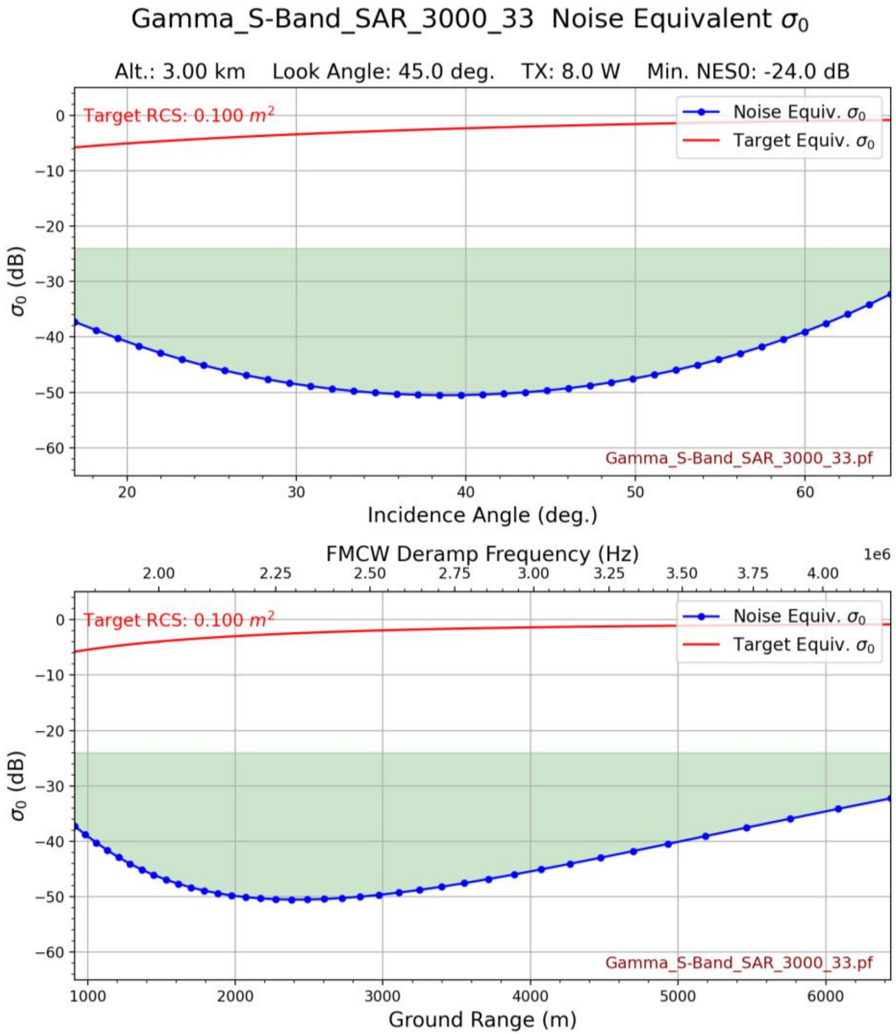

- Better that -50 dB NES0 across the swath 20→ 70 deg. look angle, 60 deg. boresight
- 3000 m altitude, long-track 120 km/h velocity (33.3 m/s)
- 8-Watt TX power, 400 MHz bandwidth
- 4.4 ms chirp (PRF = 224 Hz)
- 17–65-degree incidence angle
- 3.97 km slant-range swath, ground-range swath: 5.5 km.
- Data rate 6.25 Mbytes/s, 8 bits I, 8-bits Q.
- Receiver IF offset: 2.6 MHz

GLSAR Flight Testing in Pennsauken, NJ

- Initial test flights May 20-22, 2024
- Copper River Park, Pennsauken Township, New Jersey
- Stable UAV flight implies good quality INS and radar data
- Payload 6.2 kg, approximately 25 minutes of flight-time

Repeat-Track L-Band interferometric image, Pennsauken, New Jersey

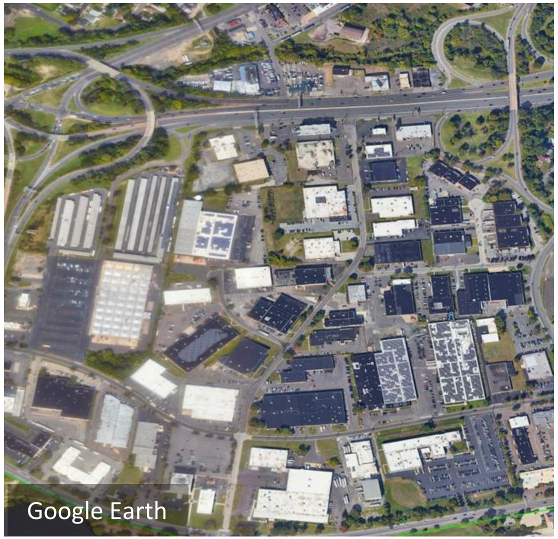

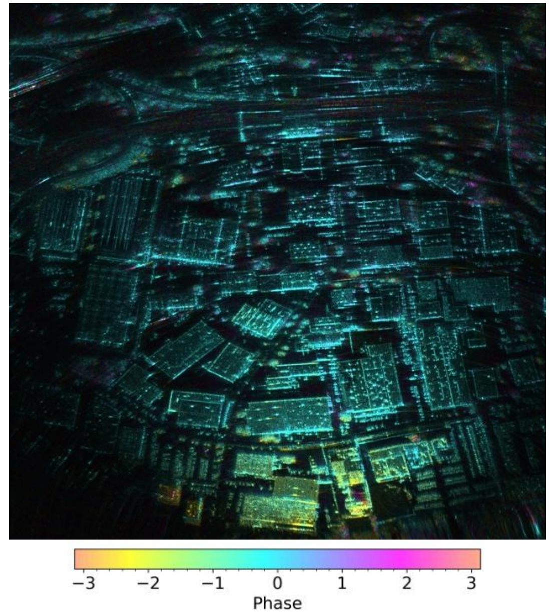

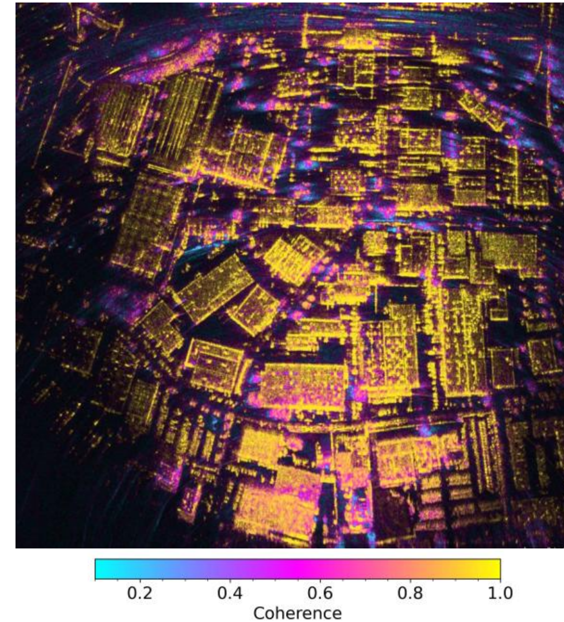

- Processed using Time-Domain Back Projection onto a latitude/Longitude grid ~50 cm spacing
- Resolution ~ 1 meter slant-range x 1m azimuth
- Time interval ~ 3 minutes

Bogie Farm, Vermont, USA: GLSAR/GSSAR Campaign 5-9 May 2025

Gamma L-Band SAR (GLSAR) on Harris HX8 UAV

Gamma S-Band SAR (GSSAR) on Harris HX8 UAV

Gamma L-Band SAR (GLSAR) on Harris HX8 UAV

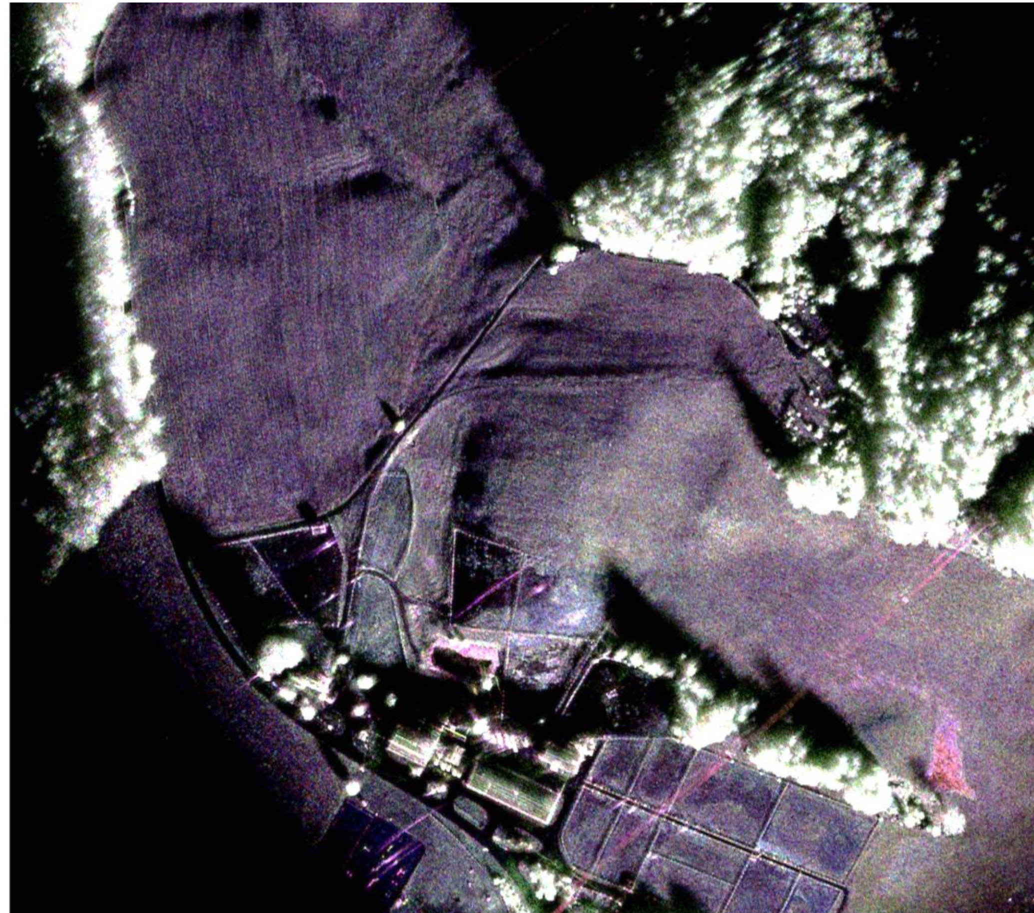

S-Band Pauli decomposition, 400 MHz bandwidth, 50-cm resolution

UAV altitude: 120 m, 1 x 1 km, Norwich, Vermont

UAV L- and S-Band Repeat-Track Interferometry

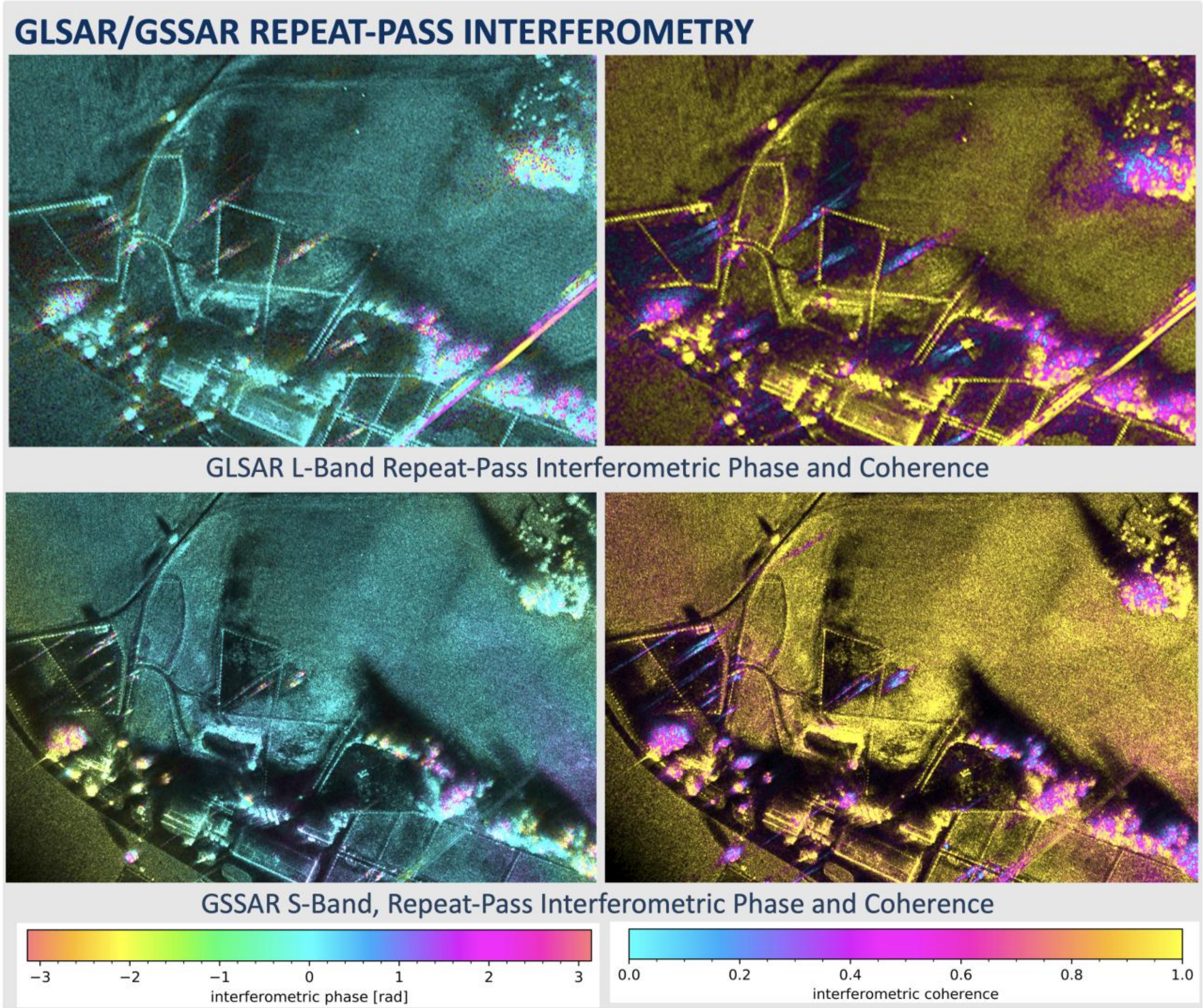

Bogie Farm, Vermont, USA: GLSAR/GSSAR Campaign 5-9 May 2026

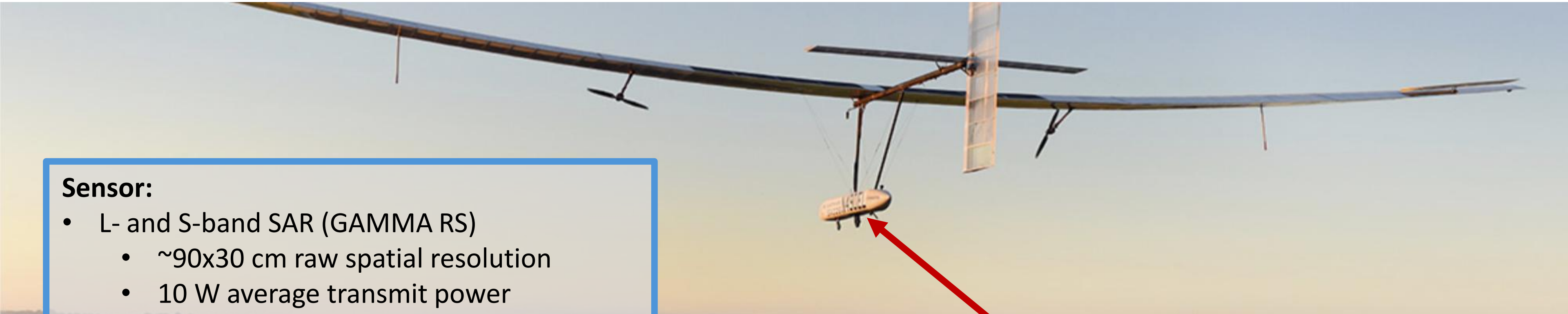

Sensor:

- L- and S-band SAR (GAMMA RS)
    - ~90x30 cm raw spatial resolution
    - 10 W average transmit power
    - 16 km swath width
    - NESZ <-24 dB
- Combined (aircraft + radar)
    - Greater flexibility on when/where/how often data are collected
    - Nominal unit cost ~US$1.5M
    - Direct tradeoff between spatial coverage and temporal resolution
    - Greenland glaciers: imagine InSAR with ~30-60 min repeat times

Just **one example** illustrating the broader potential of smaller, lighter, cheaper sensors and versatile platforms